Green Chemistry

PERSPECTIVE

View Article Online
View Journal | View Issue

Check for updates

Cite this: *Green Chem.*, 2021, **23**, 249

CO_2 hydrogenation over heterogeneous catalysts at atmospheric pressure: from electronic properties to product selectivity

Yaning Wang,[a] Lea R. Winter,[b] Jingguang G. Chen *[b] and Binhang Yan *[a]

Received 17th October 2020,
Accepted 24th November 2020

DOI: 10.1039/d0gc03506h

rsc.li/greenchem

The production of chemicals and fuels *via* chemical reduction of CO_2 by green H_2 represents a promising means of mitigating CO_2 emissions. The heterogeneous catalytic reaction of CO_2 and H_2 under atmospheric pressure primarily produces CO and CH_4, while CH_3OH and C_{2+} hydrocarbons are obtained at high pressure. Improving the catalytic selectivity improves the energy efficiency for a given yield and greatly reduces the downstream separation costs. In this work, we review the recent progress in tuning the selectivity of CO_2 hydrogenation over heterogeneous catalysts at atmospheric pressure. We describe fundamental insights into the relationships among the electronic properties of active metals, the binding strengths of key intermediates, and the CO_2 hydrogenation selectivity. The manipulation of the electronic properties, and consequently the product selectivity, can be achieved mainly by controlling the particle size, bimetallic effects, and strong metal–support interactions. Finally, we discuss challenges and opportunities for the rational design of CO_2 hydrogenation catalysts with high activity and desired selectivity.

1. Introduction

In recent decades, global warming has become an increasingly serious problem that affects human survival and development. Rising temperatures have led to many global environmental crises such as the melting of glaciers,[1] worsening wildfires,[2] and extreme weather.[3] There is considerable evidence that the excessive emission of infrared-trapping gases such as carbon dioxide to the atmosphere is indeed the primary culprit for global warming.[4,5] The CO_2 emissions are mainly contributed by the burning of fossil fuels, and since CO_2 remains in the atmosphere for hundreds of years, the concentration of atmospheric CO_2 is increasing steadily.[6,7] Thus, significant efforts are required to mitigate atmospheric CO_2 emissions.

Among the strategies for decreasing the concentration of atmospheric CO_2, the most common methods are CO_2 capture, storage, and chemical utilization. Compared with sequestration, transforming CO_2 into commodity chemicals, especially with CO_2-free H_2,[8] not only consumes CO_2 but also reduces the use of fossil-derived raw materials. The research of Tackett *et al.*[8] revealed that a process powered by electricity emitting less than 0.2 kg of CO_2 per kW per h would achieve a net reduction in CO_2, although the high price of renewable energy limits the large-scale application of the CO_2 hydrogenation processes at present. Zhang *et al.*[9] have demonstrated that the economic profit can be gained when a suitable carbon tax is implemented and the cost of renewable energy is greatly decreased in the future. Generally, a net CO_2 reduction *via* the hydrogenation processes can be achieved with the availability of low-carbon or carbon-free energy. Nowadays, thermochemical and electrochemical reductions of CO_2 represent the two main pathways of CO_2 conversion; this perspective article focuses on thermochemical methods. Although the thermal reduction of CO_2 is promising, the efficient activation of the thermodynamically stable C=O bond in CO_2 (bond energy = 806 kJ mol^{-1}) poses a major challenge. The development of highly efficient catalysts is crucial to reduce the activation barrier and hence the energy required for converting CO_2 into commodity chemicals.

Under atmospheric pressure, the products of CO_2 thermocatalytic reduction with H_2 are CO and CH_4, through the reverse water–gas shift (RWGS) reaction and methanation (also known as the Sabatier reaction), respectively:

$$CO_2 + H_2 \leftrightarrow CO + H_2O \quad \Delta H_{298^\circ C} = +41.2 \text{ kJ mol}^{-1} \tag{1}$$

$$CO_2 + 4H_2 \leftrightarrow CH_4 + 2H_2O \quad \Delta H_{298^\circ C} = -165 \text{ kJ mol}^{-1} \tag{2}$$

Conversion of CO_2 to either product with high selectivity is desired according to specific application requirements. CO can be further converted to valuable chemicals and fuels through well-developed synthesis gas conversion technologies, such as

[a]Department of Chemical Engineering, Tsinghua University, Beijing 100084, China. E-mail: binhangyan@tsinghua.edu.cn; Tel: +(86) 010-62797920
[b]Department of Chemical Engineering, Columbia University, New York, NY 10027, USA. E-mail: jgchen@columbia.edu; Tel: +(212) 854-6166

Fischer–Tropsch (FT) synthesis and methanol synthesis. The methanation reaction is widely explored as one of the potential Power-to-Gas (PtG) technologies to foster interaction of gas and electric grids, enabling the methane production (from anthropogenic captured CO_2 and renewable generated hydrogen) to be injected into the gas grid or locally used (industrial process, heating system, vehicles).

Other hydrogenation products such as methanol and C_{2+} hydrocarbons are obtained under high pressure with low yields. There are many similarities between the atmospheric-pressure and high-pressure reactions in the reaction mechanism and catalyst design, although this perspective article mainly discusses the atmospheric-pressure reactions. Most research was aimed at increasing catalytic activity to boost production. However, the demand for selective heterogeneous catalysis has become more apparent in CO_2 hydrogenation. It is of paramount importance that a molecular-level understanding of the factors that control the selectivity of a catalytic reaction from the phenomenological or "trial and error" mode into the rational design of catalysts.[10] The activity and selectivity of CO_2 hydrogenation have been demonstrated to be very sensitive to the catalyst structure.[11] Therefore, understanding catalyst structure is paramount to the rational design of heterogeneous catalysts for selective CO_2 hydrogenation.

Several articles have reviewed the progress in experimental and theoretical studies of CO_2 hydrogenation. Porosoff *et al.*[12] discussed the challenges and opportunities for CO_2 hydrogenation into CO, methanol, and hydrocarbons. Aziz *et al.*[13] summarized the progress in the development of various catalysts for CO_2 methanation. Daza *et al.*[14] compared RWGS catalysts and the corresponding reaction mechanisms. Chen *et al.*[15] reviewed single-atom catalysts and their extraordinary performance during RWGS. In addition to these reviews of experimental findings, Li *et al.*[16] provided a theoretical overview of CO_2 hydrogenation. Several other reviews focus on recent advances in a single CO_2 hydrogenation pathway, *i.e.*, CO_2 methanation,[17–21] reverse water gas shift,[22,23] or CO_2 to methanol.[24–27] In contrast, this perspective article aims to provide insight into recent developments in the competing atmospheric-pressure pathways of CO_2 methanation and RWGS. We focus on providing guidance for fine-tuning the electronic properties of active metals in order to enable the design catalysts with high selectivity and activity for CO_2 hydrogenation. Accordingly, the basic principles underlying the design and development of nanostructured catalysts also are discussed.

According to the Sabatier principle, the most active catalysts should bind adsorbates with a moderate strength: catalysts showing weak adsorbate binding energy are insufficient for activating reactants, but strong binding energy prevents product desorption. Research on reaction mechanisms has improved the development of a rationale for optimizing catalyst composition. Kattel *et al.*[28] proposed a reaction mechanism based on density functional theory (DFT) calculations (Fig. 1), suggesting that the key intermediate of CO_2 hydrogenation *via* the RWGS + CO-hydrogenation pathway or the direct C–O bond cleavage pathway is adsorbed CO. This mechanism has been verified through *in situ* characterization. For example, Heine *et al.*[29] used ambient-pressure X-ray photoelectron spectroscopy (AP-XPS) to demonstrate that the methanation reaction over Ni(111) proceeded *via* dissociation of CO_2, followed by reduction of CO to atomic carbon and its sub-

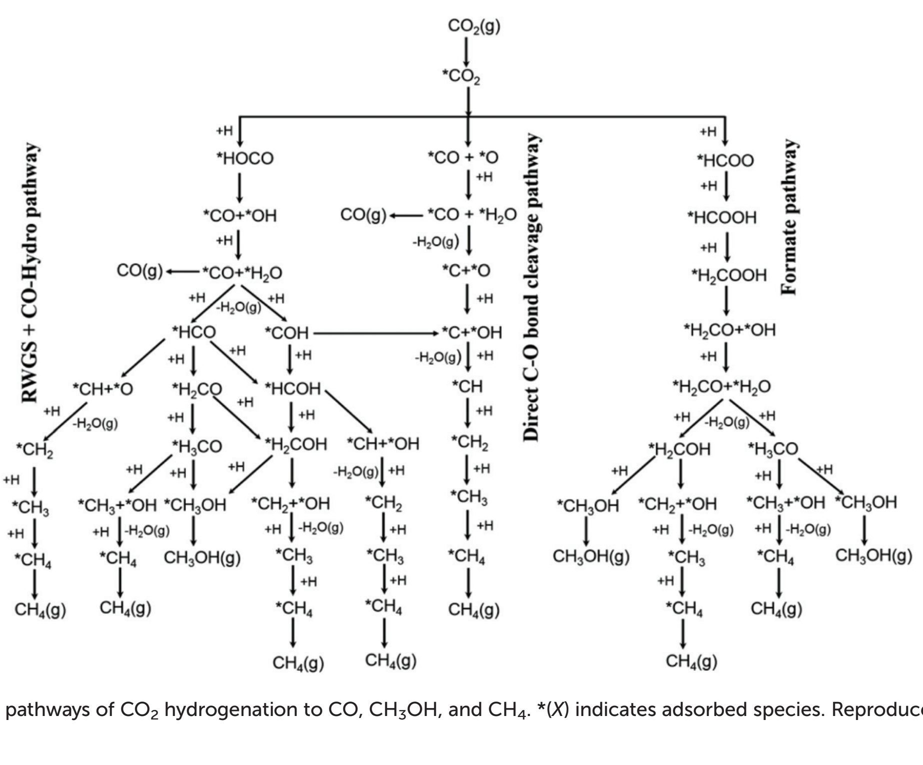

Fig. 1 Possible reaction pathways of CO_2 hydrogenation to CO, CH_3OH, and CH_4. *(*X*) indicates adsorbed species. Reproduced from ref. 28.

sequent hydrogenation to methane. Zhao *et al.*[30] unraveled the surface reaction mechanism of CO_2 hydrogenation on Ru/Al_2O_3 *via in situ* control of the individual formation and hydrogenation steps for each adsorbed species, using operando diffuse reflectance infrared Fourier transform spectroscopy (DRIFTS) combined with iterative Gaussian fitting. According to their research, CO_2 → *HCO^{3-} on the metal-support interface → *CO on the metal surface → CH_4 is the dominant reaction step. Martin *et al.*[31] observed the linearly-adsorbed CO species on reduced Rh (Rh–CO_{lin}) as the active intermediate in CO_2 methanation over Rh/Al_2O_3. According to their results, the rate-determining step for CO_2 reduction and RWGS was the conversion of *HCOO, whereas that for CH_4 formation was the hydrogenation of *CO. As shown in Fig. 1, absorbed CO serves as the key intermediate of the CO_2 hydrogenation pathways that lead to either CO or CH_4 as the final products.

In this perspective article, we focus on CO_2 hydrogenation pathways for which adsorbed CO leads to selective CO or CH_4 production. The key factor that determines the reaction pathway is the activation energy difference between CO desorption and further reaction of adsorbed CO. The adsorption strength of CO is determined by the electronic structure of the catalyst and in particular that of the active metals.[32,33] Thus, understanding and controlling the intrinsic electronic properties of the active metal is crucial to the design of catalysts with high selectivity. The electronic properties of the active metal can be tuned through the electron transfer resulting from the formation of bimetallic bonds and interactions with catalyst supports. In this work, we review recent progress in CO_2 hydrogenation at atmospheric pressure and discuss the relationship between CO binding energy and the catalytic selectivity. We summarize the effects of intrinsic electronic properties, particle sizes, bimetallic formation, supports, and other related factors on CO_2 hydrogenation selectivity. Finally, challenges and opportunities for achieving the rational design of CO_2 hydrogenation catalysts with high activity and selectivity will be discussed.

2. Intrinsic electronic properties of metal catalysts

The catalytic performance of supported catalysts is closely related to the adsorption strength and orientation of reactants, intermediates, and products, which are mainly determined by the intrinsic electronic properties of the active metal. For example, Mutschler *et al.*[34] examined a series of pristine transition metals for CO_2 hydrogenation and found that Co exhibited high activity and selectivity toward methane. Garbarino *et al.*[35] have investigated the CO_2 hydrogenation performance of unsupported Co and Ni nanoparticles. According to their research, unsupported metallic cobalt nanoparticles showed significant activity in CO_2 methanation but deactivated upon time on stream due to fast sintering and the formation of encapsulating carbon. Unsupported Ni nanoparticles exhibited weak activity in either the RWGS reaction or the methanation reaction.[36,37] In the research of Kim *et al.*,[38] unsupported Fe-oxide NPs (10 to 20 nm) were tested at 873 K, showing 85% CO selectivity and medium CO_2 conversion (~30%). According to the research of Bersani *et al.*,[39] copper nanoparticles yielded mixtures of CO and CH_4 in the temperature range of 250 °C to 500 °C. As for precious metals, Panagiotopoulou[40] revealed that the activity for CO_2 conversion over TiO_2-supported metal catalysts followed the order of Pd < Pt < Ru < Rh, where the Ru- and Rh-based catalysts favored methanation and the Pt- and Pd-based catalysts mainly produced CO. In general, the main product of atmospheric-pressure CO_2 hydrogenation over Rh-,[31,41] Ru-,[34,42–44] Co- and Ni-based[45–48] catalysts is methane, while the Pd-,[49] Fe-,[50–52] Pt-,[53–55] and Cu-based catalysts favor the RWGS reaction, as shown in Fig. 2.

A summary of the catalytic performance of several monometallic catalysts is shown in Table 1, revealing that different transition metals exhibit widely different selectivity for CO_2 hydrogenation. The electronic properties of metal catalysts, which affect the CO binding energy and the reaction selectivity, can be modified by various means in order to promote desired reaction pathways and inhibit side reactions. The methods for tuning the intrinsic catalyst performance are detailed in the following sections.

3. Particle size effect

As shown in Table 1, intrinsic catalytic performance depends on the particle size of the active metal, which correlates with metal loading (it is common for the particles to grow up with the increasing of loading). When the particles decrease to sub-nm size or even to the scale of single atoms, the methanation reaction is inhibited.[59]

In recent years, single-atom and sub-nm catalysts have been studied intensively because of their unique chemical pro-

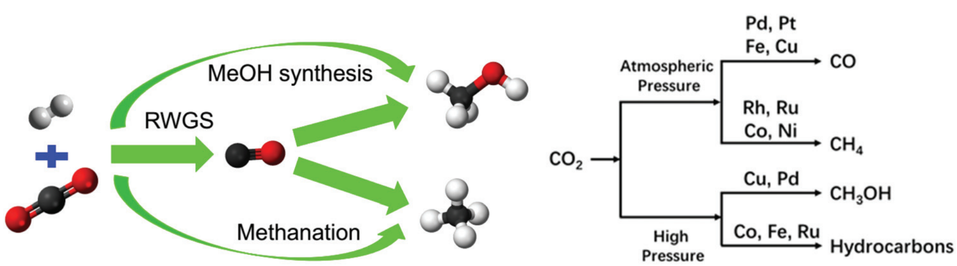

Fig. 2 Schematic showing possible products and potential catalysts for CO_2 hydrogenation.

Table 1 Summary of reaction conditions, CO_2 conversion, and selectivity for CO_2 reduction by H_2 on transition metal catalysts

Catalysts	Loading (wt%)	$H_2:CO_2$ ratio	Temperature (K)	Conversion (%)	CO Selectivity (%)	CH_4 Selectivity (%)
Ru/SiO_2 [56]	5	9 : 1	473	3.2	0.6	99.4
Ru/Al_2O_3 [34]	0.5	4 : 1	653	74.7	1.2	98.8
Ru/TiO_2 [42]	0.5	4 : 1	623	~21	14	86
Ru/CeO_2 [43]	1.8	4 : 1	573	~83	0	100
Ru/MSN[57]	5	4 : 1	623	95.7	0	100
Rh/SiO_2 [31]	3	5 : 1	723	~39	~22	~78
Rh/Al_2O_3 [41]	0.2	4 : 1	473	~98	~0	~100
Rh/TiO_2 [40]	0.5	4 : 1	623	~75	0	100
Rh/CeO_2 [49]	3	5 : 1	623	~46	0	100
Rh/MSN[57]	5	4 : 1	623	99.5	0	100
Ni[34]	—	4 : 1	793	54.7	20.1	79.9
Ni/SiO_2 [47]	6.2	4 : 1	723	36.8	18.2	81.8
Ni/SiO_2 [45]	5	4 : 1	623	27.6	11.6	85.5
Ni/SiO_2 [46]	10	4 : 1	573	42.4	3.4	96.6
Ni/SiO_2 [49]	3	5 : 1	723	~45	~54	~46
Ni/SiO_2 [56]	8.2	9 : 1	473	1	0.2	99.8
Ni/Al_2O_3 [49]	3	5 : 1	723	~5	~60	~40
Ni/Al_2O_3 [56]	8.2	9 : 1	473	2.6	0.6	99.4
Ni/TiO_2 [48]	10	4 : 1	623	~42	~24	~76
Ni/MSN[57]	5	4 : 1	623	85.4	0.1	99.9
Ni/CeO_2 [49]	3	5 : 1	623	~44	~0	~100
Pt/SiO_2 [54]	1.7	2 : 1	623	9.0	98.4	1.6
Pt/Al_2O_3 [55]	1.0	7 : 10	673	18	~100	~0
Pt/TiO_2 [54]	1.7	2 : 1	623	10.2	~100	~0
Pt/CeO_2 [53]	1	1 : 1	673	~16	~100	~0
Pd/SiO_2 [49]	3	5 : 1	723	~13	~40	~60
Pd/Al_2O_3 [49]	3	5 : 1	723	~25	~50	~50
Pd/TiO_2 [40]	0.5	4 : 1	623	~7	100	0
Pd/CeO_2 [49]	3	5 : 1	723	~51	~87	~13
Fe[34]	—	4 : 1	813	26.7	84.1	15.9
Fe/MSN[57]	5	4 : 1	623	4	8	92
Cu/TiO_2 [58]	5	3 : 1	493	0.5	83.6	16.4
Cu/ZrO_2 [58]	5	3 : 1	493	0.5	80.2	19.8
Cu/MSN[13]	5	4 : 1	623	3.3	21	79

perties and extraordinary catalytic behavior.[60] Many studies have revealed that metals that produce a mixture of methane and CO as nanoparticles show suppression of methane generation as single-atoms.[61,62] The catalytic performance of single-atom catalysts and metal nanoparticles are listed in Table 2. Compared to metal particles, single-atom catalysts not only utilize the atom more efficiently but also benefit for CO selectivity in RWGS.[11]

The underlying properties of single-atom catalysts that give rise to these unique characteristics have been widely studied.[63,64] It is generally accepted that the electron density of single-atom catalysts is changed due to the low-coordination environment and strong metal–support interaction. Single-atom catalysts are positively charged (usually noted as $M^{\delta+}$), leading to a weaker interaction with CO. Kwak *et al.*[65,66] prepared atomically-dispersed Pd/Al_2O_3 and Ru/Al_2O_3 catalysts to investigate

Table 2 Summary of reaction conditions, CO_2 conversion, and selectivity on supported transition metal catalysts with different particle sizes

Catalysts	Loading (%)	Particle size (nm)	$H_2:CO_2$ ratio	Temperature (K)	Conversion (%)	CO Selectivity (%)	CH_4 Selectivity (%)
Pd/Al_2O_3 [66]	10	~2	3 : 1	673	~40	~10	~90
Pd/Al_2O_3 [66]	0.5	SA	3 : 1	673	~20	~62	~38
Ru/Al_2O_3 [65]	2	2	3 : 1	573	—	~12	~88
Ru/Al_2O_3 [65]	0.5	SA	3 : 1	573	—	~84	~16
Ru/TiO_2 [79]	10	~2.5	4 : 1	473	<5	<2	>98
Ru/TiO_2 [79]	0.5	SA	4 : 1	473	<5	35	65
Ir/CeO_2 [69]	15	~2.5	4 : 1	573	6.9	44	56
Ir/CeO_2 [69]	5	<1	4 : 1	573	6.8	>99	<1
Ir/TiO_2 [15]	5	~2	1 : 1	623	~2.1	21.8	78.2
Ir/TiO_2 [15]	0.1	SA	1 : 1	623	~2.1	~100	~0
Pt/CeO_2 [70]	2	~1.5	12.5 : 1	723	—	0	100
Pt/CeO_2 [70]	0.5	SA	12.5 : 1	723	—	100	0
Ni/CeO_2 [50]	1.5	0.9	3 : 1	623	26.8	21.6	78.4
Ni/CeO_2 [50]	0.5	0.6	3 : 1	623	23.1	40.6	59.4
Ni/SiO_2 [71]	10	~9	1 : 1	623	~10	~10	~90
Ni/SiO_2 [71]	0.5	SA	1 : 1	623	~10	~40	~60

the influence of particle size on the CO_2 hydrogenation process. The results suggested that the RWGS reaction was the dominant reaction pathway over single-atom catalysts. The same trends were obtained using Rh/CeO_2 single-atom catalysts.[67] Matsubu *et al.*[68] investigated CO_2 hydrogenation over Rh/TiO_2 with different Rh loadings. They observed a close correspondence between the turnover frequency (TOF) of RWGS and the fraction of isolated Rh sites, as shown in Fig. 3. A similar result was obtained by Li *et al.*[69] As shown in Fig. 4, the CO selectivity increased as the Ir loading amount decreased. In addition to achieving high selectivity toward CO, single-atom catalysts also show extraordinary activity. Wang *et al.*[70] compared the difference between 0.5 wt% Pt single-atom and 2 wt% Pt nanocluster catalysts on CeO_2 during CO_2 hydrogenation. The activity results indicated that the single-atom catalysts exhibited a more than 7-fold increase in rate compared with the nanoclustered catalyst and with 100% CO selectivity. The authors demonstrated that the weak binding between isolated Pt atoms and CO restricted the further hydrogenation of CO.

The same trend that single-atom or sub-nanometer catalysts favor CO formation also has been observed over non-precious metal catalysts. However, the synthesis of highly-dispersed non-precious metal catalysts is much more difficult than the preparation of precious-metal single-atom catalysts. In general, metals are highly dispersed on the support at low metal loadings, whereas the metal particles aggregate at high metal loadings, forming large particles. Therefore, small clusters or single-atom catalysts are usually synthesized by reducing metal loading (≤0.5%).

Applying this method, Wu *et al.*[71] compared the catalytic performance of 0.5 wt% Ni/SiO_2 and 10 wt% Ni/SiO_2. The authors proposed a consecutive reaction pathway (intermedi-

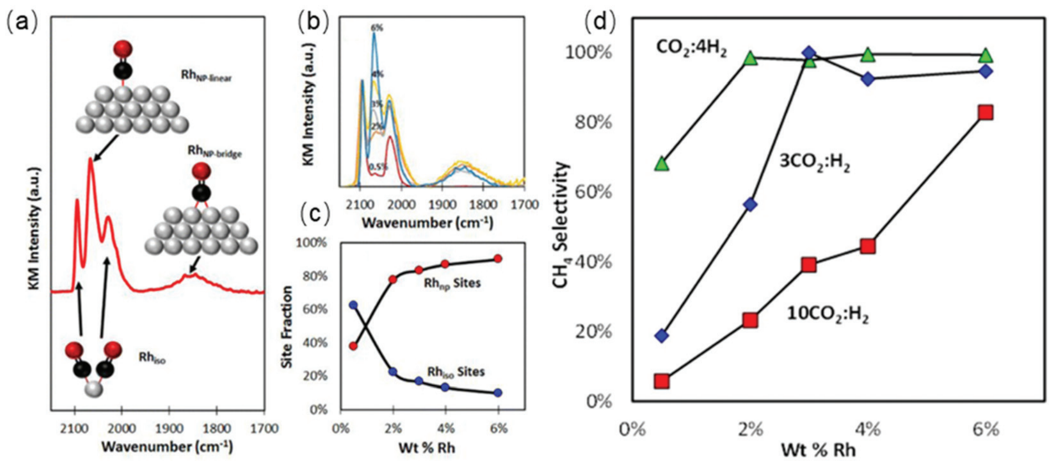

Fig. 3 (a) DRIFT spectrum obtained from a saturated layer of CO adsorbed at 300 K on 4% Rh/TiO_2. Insets show ball-and-stick models of assigned vibrational modes. (b) DRIFT spectra of CO on all five weight loadings of Rh/TiO_2 catalysts. The spectra are displayed in Kubelka–Munk (KM) units and normalized by the symmetric *gem*-dicarbonyl peak (2097 cm^{-1}) height to allow for comparison. (c) Site fraction (%) of isolated (Rh_{iso}) and nanoparticle-based Rh sites (Rh_{NP}) as a function of wt% Rh. (d) CH_4 selectivity as a function of wt% Rh for 0.25, 3, and 10 $CO_2 : H_2$ feed ratios measured at 200 °C.

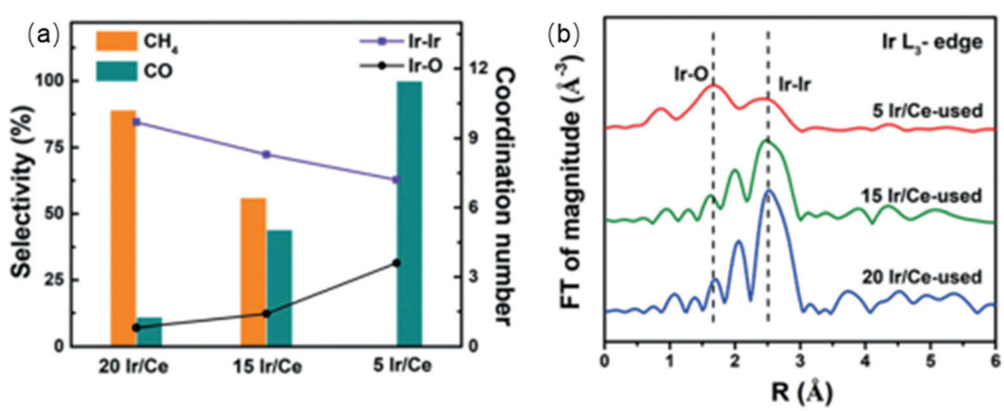

Fig. 4 (a) The coordination number of Ir–Ir and Ir–O shells (line graph, right axis) relative to catalyst selectivity (bars, left axis) for CO_2 hydrogenation over Ir/Ce catalysts with different Ir loadings. (b) Ir L_3-edge Extended X-ray Absorption Fine Structure (EXAFS) of the Ir/Ce-used catalysts. Reproduced from ref. 69.

ates → CO → CH_4) and a parallel pathway (intermediates → CO and intermediates → CH_4). The reactants underwent consecutive pathways over small Ni particles and both consecutive and parallel pathways over larger particles. The consecutive pathway is associated with low H_2 coverage on the Ni surface, which leads to the dissociation of formate intermediates and results in CO formation and high CO selectivity. Lu *et al.*[72,73] demonstrated that monodispersed NiO/CeO_2 and NiO/SBA-15 catalysts exhibited 100% CO selectivity regardless of the reaction temperature. Gonçalves *et al.*[74] employed magnetron sputtering deposition to prepare small Ni nanoclusters on SiO_2 and reached the same conclusions that small Ni particles tended to produce CO rather than methane. The relationship between selectivity and the Ni electronic properties was investigated by Vogt *et al.*[75] Through operando quick X-ray absorption spectroscopy (Q-XAS), the authors suggested that sub-2 nm Ni particles exhibited lower d-band energy or higher electron localization than large nanoparticles, which had a considerable impact on the catalytic activity.

The enhanced CO selectivity using single-atom catalysts also was demonstrated by theoretical calculations. Yan *et al.*[76] illustrated that the RWGS route was more energetically favorable over monolayer Ru sites with a relatively low energy barrier for CO_2 activation and CO formation, while methanation was favored over 3D Ru nanoclusters. Chen *et al.*[15] combined experimental data with DFT calculations to investigate single-atom catalysts for CO_2 hydrogenation. Single-atom Ir/TiO_2 exhibited 100% selectivity toward CO due to the low coordination number of Ir. The authors demonstrated that the desorption energy of CO was lower than the dissociation barriers of the intermediates for single-atom Ir/TiO_2, Pt/TiO_2, and Au/TiO_2 catalysts. As displayed in Fig. 5, the DFT calculation results correlated well with the experimental data over a series of catalysts.

While single-atom catalysts demonstrate promising activity and selectivity for CO_2 hydrogenation, the instability of single atoms poses a major challenge for practical applications.[76–78] Single-atom active metals tend to agglomerate into larger particles during the reaction, especially at high temperatures. Therefore, the observed decline of catalytic activity and CO selectivity is ascribed to the sintering of the single atoms. Currently, the synthesis of single-atom catalysts with high thermal stability and sintering resistance remains challenging.

Overall, the CO_2 hydrogenation selectivity varies with the metal particle size. The methanation selectivity gradually decreases as the particle size decreases until the electronic properties of the metal become altered due to the electron transfer. Notably, when the particle size decreases to the sub-nm and even single-atom scale, the metals become positively charged and the exhibits high CO selectivity.

However, except for the electron properties, there are other factors that have impact on CO_2 hydrogenation performance. Control of nanoparticle shape and size will ultimately determine the dominant surface-active terrace, edge, and corner sites. However, the geometric effect of catalysts in CO_2 hydrogenation reaction is quite complicated, and different authors have drawn different conclusions. DFT calculations showed a stronger backdonation from the metal atoms to the 2π* antibonding of adsorbed CO on low coordinated surface atoms (corners and edges).[80] Martins *et al.*[81] found that high CH_4 selectivity was favored in the presence of small particles with a majority of surface sites being edges and corners. However, Loveless *et al.*[82] demonstrated that the corner sites were less active due to the lack of vacancies required for H-assisted hydrogenation paths. The catalytic investigation of Beierlein *et al.*[83] showed that CO_2 methanation on Ni–Al_2O_3 was a structure–insensitive reaction and terrace atoms were the active sites. Additionally, the H-spillover effect also should be taken into accounts. Guo *et al.*[84] demonstrated the methanation activity was determined jointly by strong metal–support interactions and H-spillover effects, suggesting a more complex relationship between particle size and selectivity. The strong metal–support interactions between single Ru atoms and CeO_2 suppressed the activation of carbonyls, while the significant H-spillover effects over large Ru nanoparticles greatly hindered the removal of H_2O – conditions which are both unfavorable for methanation. As displayed in Scheme 1, the methanation activity reached a maximum over intermediate-sized Ru nanoparticles when both factors were taken into account.

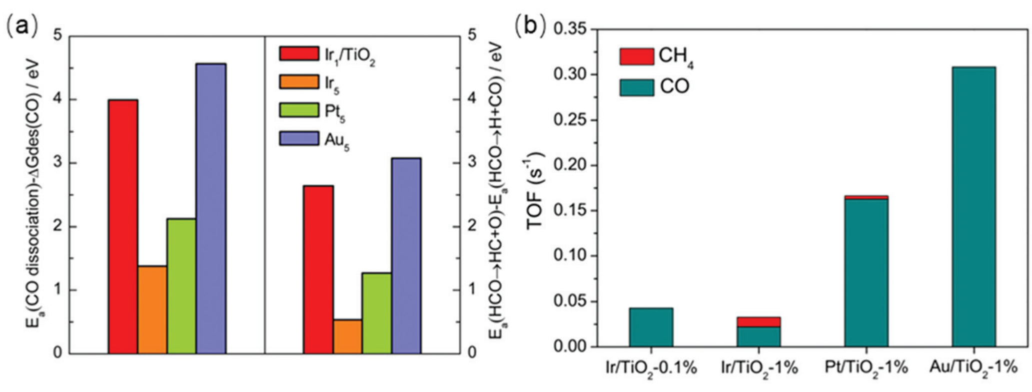

Fig. 5 (a) (Left) Difference between activation energies E_a for CO dissociation and desorption free energies of CO. (Right) Difference in activation energies between HCO → HC + O and HCO → H + CO on Ir_1/TiO_2 and stepped Ir_5, Pt_5, and Au_5 surfaces. (b) Calculated TOFs for RWGS and methanation reactions on Ir/TiO_2-0.1%, Ir/TiO_2-1%, Pt/TiO_2-1%, and Au/TiO_2-1% catalysts. Reproduced from ref. 15.

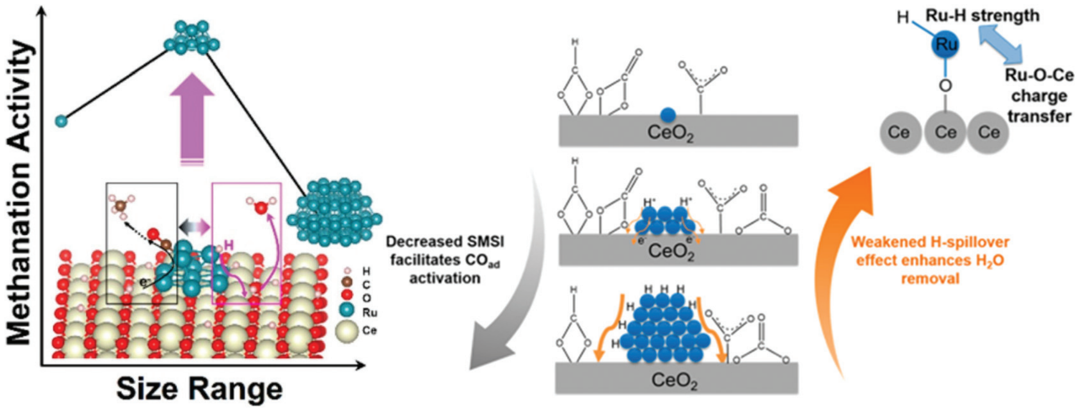

Scheme 1 Competitive strong metal–support interactions (SMSI) and H-spillover effect lead to competing CO activation and surface dehydration for CeO_2-supported single Ru atoms, Ru nanoclusters, and large Ru nanoparticles. Reproduced from ref. 84.

4. Bimetallic effect

The introduction of a second metal is another effective way to tune the electronic properties of the active metal. The electron transfer between the two metals modifies the electronic properties of the active metal and changes the selectivity of the products. For example, the introduction of typical methanation metals such as Rh, Ru, Co, and Ni to a catalyst improves the methane selectivity. Liu *et al.*[85] found that the bimetallic NiCo/Al_2O_3 catalysts exhibited enhanced methanation activity and stability compared to monometallic Ni/Al_2O_3. Xu *et al.*[86] revealed that the addition of Co to Ni/Al_2O_3 decreased the activation energy of methanation. Bimetallic Ni–Rh/$LaAlO_3$ achieved a 52% enhancement in the methanation turnover frequency [13.9 mol (mol h)$^{-1}$] compared to Rh/$LaNi_{0.08}Al_{0.92}O_3$ [9.16 mol (mol h)$^{-1}$].[87] Shang *et al.*[88] and Liu *et al.*[89] demonstrated that the addition of Ru boosted the methanation yield of Ni-based catalysts.

According to the literature,[37,50,90–94] the effect of Fe addition on Ni-based catalysts is quite complicated. Mebrahtu *et al.*[92] reported that CH_4 selectivity continuously decreased as the Fe content increased in FeNi bimetallic catalysts. Results from Winter *et al.*[50] showed that a bimetallic FeNi catalyst with a 3 : 1 molar ratio of Ni to Fe exhibited comparable activity to a monometallic Ni catalyst but improved CO selectivity. The Fe K-edge X-ray absorption near edge structure (XANES) spectra in Fig. 6 revealed that Fe in the bimetallic Ni_3Fe_1 and Ni_3Fe_3 catalysts was less oxidized than that in the monometallic Fe_3 catalyst. They elucidated that the metallic Ni enhanced H_2 dissociation and facilitated spillover of atomic hydrogen, which in turn promoted the reduction of Fe oxides in the Ni–Fe catalysts. The synergetic effect of Fe and Ni in ZrO_2-supported bimetallic catalysts was investigated through DFT calculations and *in situ* DRIFTS by Yan *et al.*[94] As the scanning transmission electron microscopy with electron energy loss spectroscopy (STEM-EELS) analysis displayed in Fig. 7, Fe tended to precipitate on the surface of Ni particles. The theoretical calculations and experimental observations indicated that CH_4 was formed mainly *via* the RWGS + CO-hydrogenation pathway with *CO as a key intermediate. The interaction of *CO with

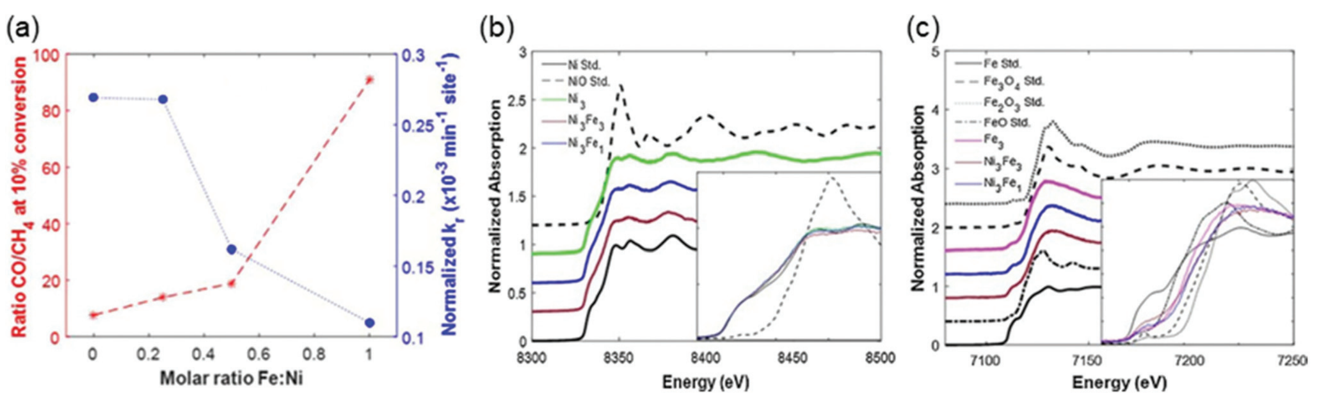

Fig. 6 (a) Summary of activity based on reaction rate constants normalized by catalyst mass and number of active sites, and selectivity based on the ratio of CO/CH_4 produced at the time of 10% conversion of CO_2 by H_2, for varying molar ratio of Fe : Ni in bimetallic FeNi/CeO_2 catalysts. X-ray absorption near edge structure (XANES) spectra of (b) the Ni K-edge for CeO_2-supported Ni_3, Ni_3Fe_3, and Ni_3Fe_1 catalysts with metallic and oxidized Ni reference standards, and (c) the Fe K-edge for Fe_3, Ni_3Fe_3, and Ni_3Fe_1 catalysts with metallic and oxidized Fe reference standards. Insets focus on the near edge region with the pre-edge normalized to zero for all spectra. Reproduced from ref. 50.

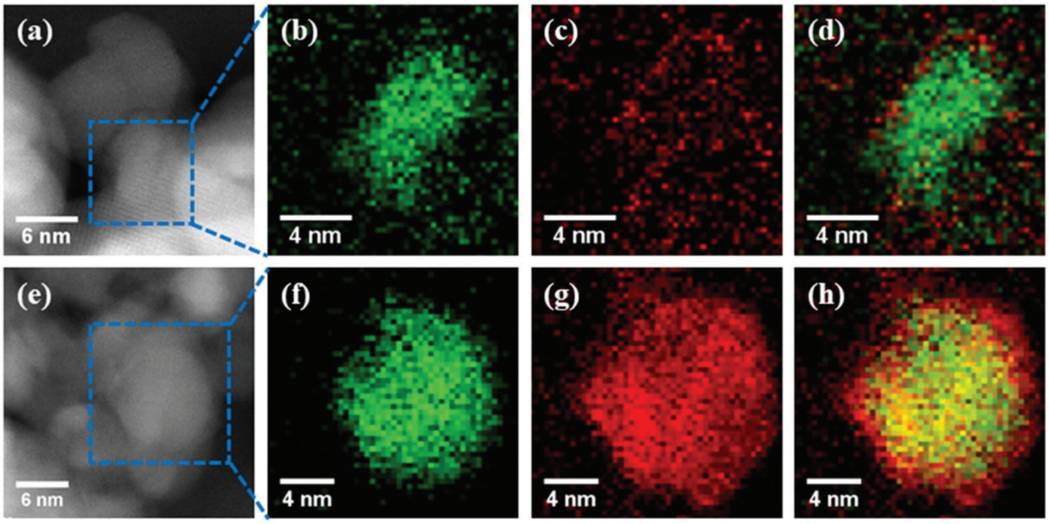

Fig. 7 Annular dark-field (ADF)-STEM images and corresponding EELS elemental maps of the spent Ni_3Fe_3/ZrO_2 and Ni_3Fe_9/ZrO_2 samples: (a) ADF-STEM image of Ni_3Fe_3/ZrO_2, (b–d) Ni (green), Fe (red), and mixed maps in Ni_3Fe_3/ZrO_2; (e) ADF-STEM image of Ni_3Fe_9/ZrO_2, (f–h) Ni (green), Fe (red), and mixed maps in Ni_3Fe_9/ZrO_2.[94]

the Ni–ZrO_2 interface was revealed to be strong enough to facilitate further *CO hydrogenation to CH_4, while the weak interaction of *CO on the Ni–FeO_x interface enabled CO desorption as the product.

In addition to changing the electronic properties, the introduction of a second metal also plays an important role in enhancing the metal dispersion and contributes to the activation of the reactants. Mihet *et al.*[95] concluded that the CO_2 conversion of Al_2O_3-supported catalysts was enhanced in the series: Ni–Pd ≥ Ni–Pt > Ni and methane selectivity followed the trend: Ni–Pt ≥ Ni–Pd > Ni. The authors attributed the promotion effect to the enhancement of metal dispersion and the improvement of NiO reducibility. Beaumont *et al.*[96] revealed that the individual Pt nanoparticles next to Co nanoparticles supported on silica enhanced the methanation activity. *In situ* XANES measurements during the reduction of the Co NPs showed that the addition of Pt NPs significantly enhanced the reduction of Co. The hydrogen atoms dissociated on Pt were transferred to the Co NPs *via* long-distance hydrogen atom spillover,[97] as shown in Scheme 2. The results of DFT calculations conducted by Ou *et al.*[98] provided theoretical insight into the promotion effects of Pt in bimetallic catalysts. The authors found that introducing Pt to Ni(111) facilitated the chemisorption of gaseous carbon dioxide.

Alkali and alkaline earth metals have promoter effects on CO_2 hydrogenation as well. Bacariza *et al.*[99] tested the effect of the addition of a series of alkaline cations into Ni/USY zeolites. The results showed that the order of improvement of the methanation activity was $Cs^+ > Na^+ > Li^+ > K^+$ for the monovalent cations and $Mg^{2+} > Ca^{2+} > Ba^{2+}$ for the divalent cations. The impregnation of 0.9–2.5% Mg on a 4.8% Ni/USY considerably improved the dispersion of Ni^0 and increased the CO_2 conversion up to 15% higher than that for the unpromoted 4.8% Ni/USY. Büchel *et al.*[100] investigated the effect of Ba and

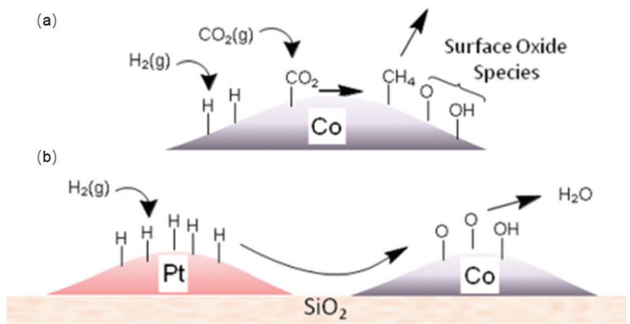

Scheme 2 (a) Production of surface oxide species from CO_2 hydrogenation and (b) transfer of adsorbed hydrogen from Pt to Co *via* a spillover mechanism to re-reduce the cobalt oxide surface, releasing water.[96]

K addition to Rh/Al_2O_3 catalysts on CO_2 hydrogenation. Below 440 °C, Rh/Al_2O_3 exhibited 100% CH_4 selectivity while K-promoted catalysts shifted to 100% CO selectivity. The change in selectivity was ascribed to the effect of Ba and K on the Rh(0)/Rh(I) ratio and on the adsorption behavior, according to the DRIFTS and CO adsorption measurements. Heyl *et al.*[101] revealed that the addition of K to Rh/Al_2O_3 affected the adsorption sites of CO on Rh and influenced the catalyst's ability to activate H_2. Thus, more facile desorption of adsorbed CO from the catalyst surface was favored and the methanation of CO was hindered. Porosoff *et al.*[102] modified $Mo_2C/\gamma\text{-}Al_2O_3$ with a K promoter and observed a significant enhancement in CO selectivity and yield. Liang *et al.*[103] and Yang *et al.*[104] provided insights into the influence of K modification by comparing K-promoted Pt/mullite and Pt/L catalysts. Their results revealed that the formation of Pt–O(OH)–K interfacial sites promoted CO desorption, thus preventing the further hydrogenation of CO to methane.

5. Support effect

The catalytic performance of supported catalysts is not only determined by the active metal but also affected by the support materials. Catalyst supports provide certain structural and physicochemical properties that ensure that the active metals remain well-dispersed. During CO_2 hydrogenation reactions, the support also participates in the adsorption and activation of CO_2. Thus, the reducibility and basicity of the support play an important role in the catalytic behavior. Dreyer *et al.*[105] selected Al_2O_3 as a representative irreducible support, ZnO and MnO_x as representative neutral reducible oxides, and CeO_2 as a representative basic reducible support to investigate the influence of support reducibility and basicity on catalytic behavior. The trend of CO_2 conversion over the pristine supports followed the strength of the support basicity as determined with CO_2 temperature-programmed desorption (TPD), following in the order of ZnO > CeO_2 > MnO_x > Al_2O_3. For pristine supports, the CO_2 conversion was determined by the ability of the materials to activate CO_2. Loading metals onto the supports changed the activity trend due to the interaction between the support and the active metal. After the addition of Ru, the CO_2 conversion and CH_4 selectivity followed the order of Ru/CeO_2 > Ru/Al_2O_3 > Ru/MnO_x > Ru/ZnO. Díez-Ramírez *et al.*[106] studied the effect of the support on Co-catalyzed CO_2 hydrogenation. The authors reported that methane selectivity followed the order of Co/CeO_2 (96%) > Co/ZnO (54%) > Co/Ga_2O_3 (53%) ~ Co/ZrO_2 (53%) at 573 K. The enhanced methanation activity of Co/CeO_2 catalysts was mainly ascribed to its superior reducibility linked to Co–ceria interactions. According to results from Muroyama *et al.*,[107] CH_4 yield over supported Ni catalysts at 523 K followed the trend of Ni/Y_2O_3 > Ni/Sm_2O_3 > Ni/ZrO_2 > Ni/CeO_2 > Ni/Al_2O_3 > Ni/La_2O_3 and the catalytic activity could be partly explained by the basic property of the catalysts.

In general, reducible metal oxide supports, such as CeO_2 and ZrO_2, activate CO_2 effectively through the metal oxide redox cycles. Since the oxygen vacancies generated by the reducible supports favor CO_2 adsorption and activation, many studies have illustrated that employing a reducible metal oxide support improves the catalytic performance.[45,109–112] The beneficial effect of Zr and Ce doping on the catalytic activity and stability has been ascribed to the enhancement of the concentration of oxygen vacancies and oxygen mobility.[113,114] Winter *et al.*[108] conducted isotope exchange studies using $C^{18}O_2$ in a batch reactor equipped with Fourier transform infrared spectroscopy and mass spectrometry to determine the involvement of surface and lattice oxygen of CeO_2 in CO_2 hydrogenation reaction. The results in Fig. 8 suggested that oxygen was exchanged by both simple heteroexchange (between one oxygen atom of a gas-phase molecule and one oxygen atom of the oxide support) and multiple heteroexchange (between an oxygen-containing gas-phase molecule and at least two oxygen atoms of the support) mechanisms. The exchange appeared to occur in two steps, where one oxygen atom in CO_2 was exchanged rapidly, and the exchange of the second oxygen atom occurred subsequently for some of the singly-exchanged $C^{16}O^{18}O$ molecules. Nie *et al.*[115] provided theoretical insights into the effect of supports (ZrO_2 and Al_2O_3) on the adsorption and activation of key species. DFT results showed that the binding energies of CO_2, H_2, and CO on Co_4/ZrO_2(111) are stronger than those on Co_4/Al_2O_3(110), in agreement with experimental TPD results. The reducibility and oxygen mobility of the supports can be promoted further by using a CeO_2–ZrO_2 solid solution, which has exhibited enhanced activity with respect to CeO_2 and ZrO_2.[116–118]

The chemical properties of the supports are influenced by many parameters, such as the morphology and the crystal phase. Different morphologies of a support with a specific crystal surface exposed exhibit distinct activity and selectivity.[119,120] Sakpal *et al.*[121] compared Ru/CeO_2 catalysts with different morphologies in the methanation reaction. Compared to cubes and octahedras, Ru/CeO_2 nanorods containing more oxygen vacancies showed higher activity in CO_2 methanation. As reported by Lin *et al.*,[122] Ru supported on rutile TiO_2 exhibited higher activity than on anatase TiO_2. Electron microscopy measurements revealed that RuO_2 was prone to sintering on anatase TiO_2 but became more dispersed on rutile TiO_2.[123] Therefore, rutile TiO_2-supported catalysts exhibited much higher activity and thermal stability for CO_2 methanation than those supported on anatase TiO_2.[124,125]

The preparation methods used for the supports also affect methanation activity. The pretreatment temperature was found to affect the density and strength of the acid sites and methanation activity of Ni/Nb_2O_5.[126] Over Ru/rutile TiO_2, the TOF values increased significantly, from 0.26 s^{-1} to 1.59 s^{-1}, with increasing pretreatment temperature.[127] The enhanced methanation activity resulted from the increase in the extent of encapsulation of Ru particles by TiO_x layers and in the amount of hydroxyl groups on the TiO_2 surface, which facilitated CO_2 dissociation. Zhang *et al.*[128] observed that selectivity toward CO over Ir/TiO_2 catalysts increased with the reduction temperature, as shown in Fig. 9. Ir/TiO_2 catalysts reduced at temperatures lower than 300 °C exhibited complete methanation of CO_2 conversion, while samples reduced beyond 600 °C led to complete CO formation. The reduced TiO_x species that originated from SMSI played a crucial role in tuning the product selectivity. Moreover, catalysts derived from a metal–organic framework (MOF) template exhibited a specific activity towards methanation.[129] Ru/ZrO_2 derived from a Ru/UIO-66 material exhibited better methanation activity and selectivity than impregnated Ru/ZrO_2 due to the high specific surface area of UIO-66.[130]

In summary, support materials influence CO_2 hydrogenation activity and selectivity due to their role in the activation of CO_2. The basic and reducible metal oxide supports usually show greater activity toward CO_2 activation. The supports also contribute to tuning the electronic properties of the active metals through metal-support interactions: the electron transfer between the active metal and support modifies the binding

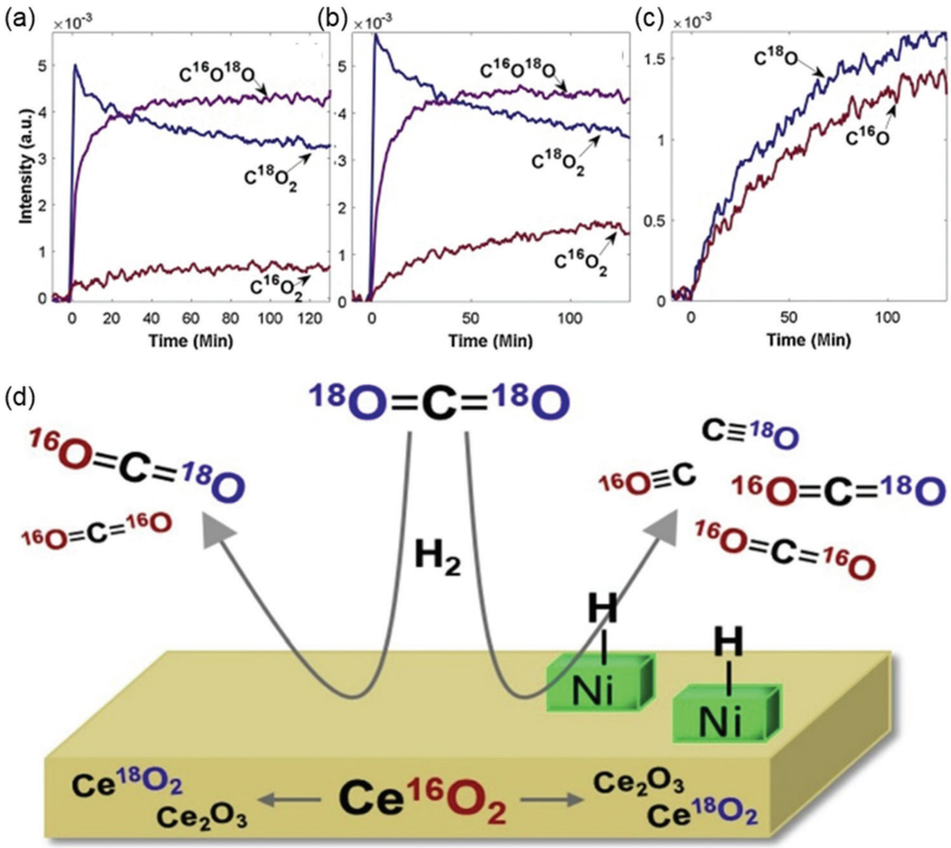

Fig. 8 The evolution of CO_2 isotope peaks over time during the reaction of $C^{18}O_2$ and H_2 over (a) blank CeO_2 and (b) 0.5% Ni/CeO_2. The separable peaks for each isotope were monitored for $C^{18}O_2$ (3510 cm^{-1}), $C^{16}O^{18}O$ (3583 cm^{-1}), and $C^{16}O_2$ (3729 cm^{-1}). (c) The evolution of CO isotope gas concentrations (monitored for $C^{18}O$ at 2070 cm^{-1} and for $C^{16}O$ at 2170 cm^{-1}) over time during the reaction of $C^{18}O_2$ and H_2 over 0.5% Ni/CeO_2. (d) Oxygen exchange between CO_2 and CeO_2 support (both the surface and lattice oxygen) under CO_2 hydrogenation conditions. Reproduced from ref. 108.

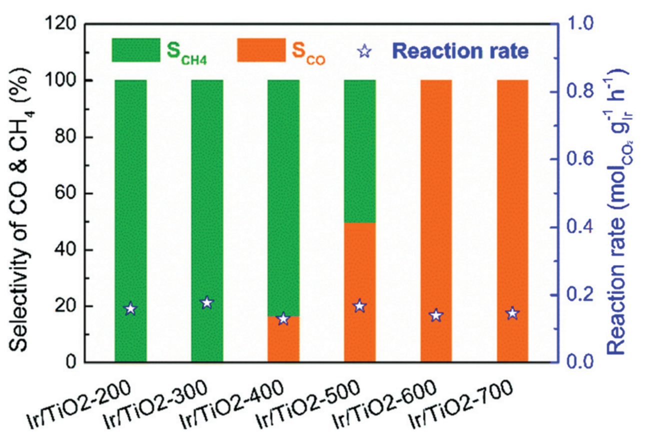

Fig. 9 Catalytic performance of the series of Ir/TiO_2-x catalysts for CO_2 hydrogenation reactions. Reaction conditions: 280 °C, 0.1 MPa, space velocity = 9000 mL h^{-1} g_{cat}^{-1}, and $H_2/CO_2/N_2$ = 70/20/10. X refers to the reduction temperature in °C.[128]

strength of CO. In addition, the specific interfacial sites between the active metal and the support also modify the catalyst selectivity.[131–133]

6. Other effects

In addition to controlling the materials and structural characteristics of the active metals and supports, there exist other methods for modifying the electronic properties of the catalyst. Electrons generated by the photoelectric effect can improve the electron density. Kim *et al.*[134] revealed that Rh- and Ru-based catalysts exhibited enhanced methane yields under light irradiation. As shown in Fig. 10, the CO_2 conversion was 1.6% at 150 °C without light on Ru, but the conversion increased to 32.6% at 150 °C with light. Other metals, such as Pt, Ni, and Cu, showed no difference with or without light irradiation.

In addition to generating emitted electrons from the active metals, the photoelectric effect also can induce electron emissions from the supports. Lin *et al.*[135] exhibited the effect of visible light on methanation over Ru/TiO_2. As a result of the photoelectric effect, the TiO_2 support generated electrons that were transferred to the Ru particles, increasing the surface electron density of Ru and consequently promoting the activation of CO_2. Doping nitrogen into TiO_2 further improved the photoelectric effect, thus promoting methanation more effectively under visible light. However, this method is only appli-

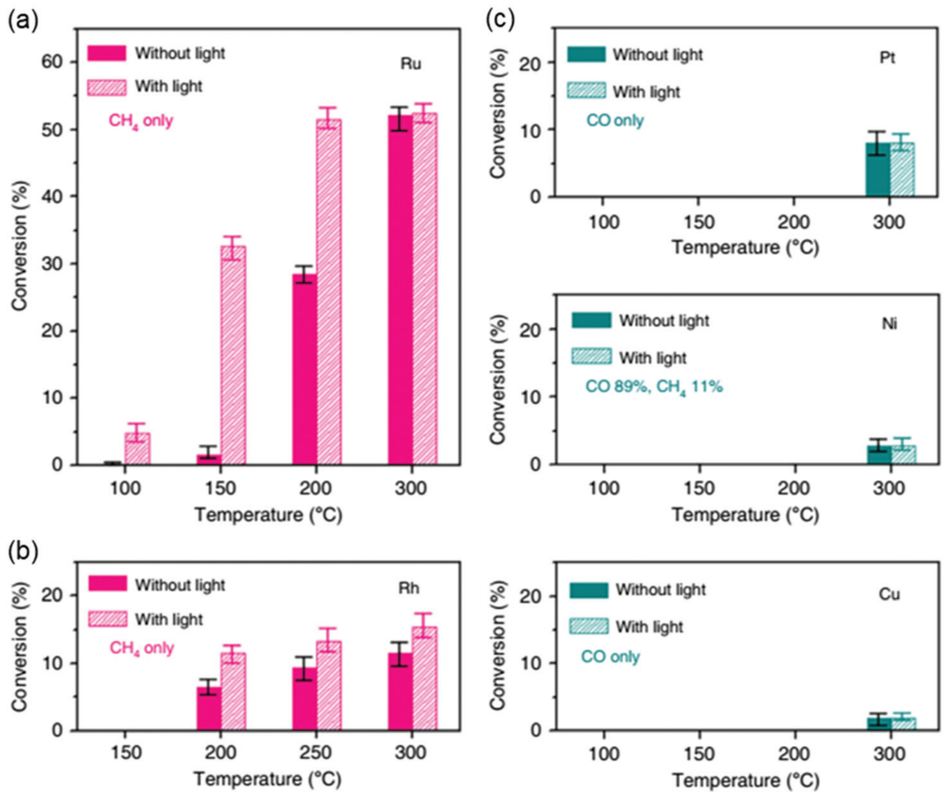

Fig. 10 Light enhancement effects on the CO_2 hydrogenation activity of metal catalysts. CO_2 conversion on (a) Ru, (b) Rh, and (c) Pt, Ni, and Cu catalysts deposited onto silica with (solid bars) and without (hatched bars) light irradiation.[134]

cable to materials with a significant photoelectric effect under visible light irradiation.

Another method of tuning the electronic properties is to derive the catalysts with higher valence state from the structured catalysts such as perovskites. Zhao *et al.*[136] reported that the CO_2 hydrogenation selectivity could be tuned by controlling the valence state of nickel using lanthanum–iron–nickel perovskites through a doping-segregation process. The higher valence states of nickel weakened the binding of CO, increasing the activation barrier for further CO hydrogenation and leading to a higher CO selectivity than that obtained with metallic nickel.

In addition to the structural and electronic properties of the catalyst, other species involved in the reaction, such as water, can affect the promotion or inhibition of CO desorption. The introduction of water vapor decreased the CO_2 conversion because H_2O inhibited CO_2 activation, reducing the amount of CO adsorbed on Ru sites.[137] Therefore, these results suggest that strategies for *in situ* water removal – such as sorption-enhanced processes or membrane reactors – may improve CO_2 conversion and merit further investigation.

Changing the coordination environment of the active metal through targeted synthesis also influences the electronic properties. Arandiyan *et al.*[138] synthesized mesoporous Rh (*meso*-Rh) nanoparticles by a soft template method to obtain a large distribution of atomic steps. In contrast with Rh nanoparticles prepared by a simple wet chemical reduction, the *meso*-Rh with low coordination atoms favored methanation over RWGS.

7. Challenges and opportunities

Thermocatalytic reduction of CO_2 by green H_2 represents a promising strategy for producing chemicals and fuels using CO_2 as an environmentally–friendly carbon source. This perspective article presents recent advances in atmospheric-pressure CO_2 hydrogenation to CO and CH_4 with a focus on the electronic properties of heterogeneous catalysts. The key descriptor of CO_2 hydrogenation selectivity is the binding energy of the key intermediate (*e.g.*, CO), which is closely related to the electronic properties of the active metal. The intrinsic properties, particle size, bimetallic effects, and metal–support interactions are critical factors that influence the electronic properties of the active metal and, therefore, the hydrogenation selectivity. Generally, catalysts with high electron density adsorb CO strongly, leading to the further hydrogenation of CO into CH_4, while catalysts with low electron density favor CO desorption.

For the selective hydrogenation of CO_2 over heterogeneous catalysts, significant challenges and research opportunities remain the following areas:

7.1. Identifying key reaction intermediates for tuning selectivity

As discussed earlier, CO is the most important intermediate in the selective catalytic hydrogenation of CO_2 to CO and CH_4. The product selectivity correlates well with the CO binding energy, which is determined by the electronic properties of the active metal. Catalysts with a weaker CO binding energy favor CO formation (*e.g.*, NiFe/ZrO_2, $LaFe_{0.9}Ni_{0.1}O_3$, *etc.*) while those with a stronger CO binding energy favor CH_4 synthesis (*e.g.*, Ni/ZrO_2, Ni/CeO_2, *etc.*). For the selective hydrogenation of CO_2 to methanol and other hydrocarbons, the identification of key reaction intermediates is critical for controlling the selectivity for the desired product. Therefore, future research efforts should focus on identifying the correct intermediate(s) for promising heterogeneous catalysts.

7.2. Stabilizing key intermediates for CH_4/CH_3OH/hydrocarbons synthesis

For direct CH_4/CH_3OH/hydrocarbons synthesis at elevated pressure, the stabilization of key intermediates is necessary for increasing the selectivity of the desired product. Therefore, significant work remains for identifying key intermediates and developing catalysts whose interactions with those intermediates facilitate further hydrogenation to the desired products. Future research in this area might aim to identify optimized $M^{\delta-}$ catalysts that selectively promote CO_2 to CH_4, CH_3OH, or long-chain hydrocarbons. Through electron transfers from supports and other metals to the active metal, the realization of $M^{\delta-}$ catalysts is potentially possible, which would improve the catalytic performance for the CO_2-to-CH_4/CH_3OH/hydrocarbons processes. Recently, negatively charged Au species ($Au^{\delta-}$) were found in Au/TiO_2 as a result of the electron migration of anatase–TiO_2 onto the metal surface due to the SMSI effect.[139,140] The $Au^{\delta-}$ catalysts exhibited enhanced catalytic activity toward CO oxidation and the water–gas shift reaction. Electron-rich $Ni^{\delta-}$ species were also observed through electron transfer from Ti and O on the anatase TiO_2 surface to atomically dispersed Ni.[141]

7.3. Promoting CO desorption for RWGS

Low-cost $M^{\delta+}$ catalysts. Metals that bind CO more strongly tend to produce CH_4/CH_3OH/hydrocarbons whereas metals with higher valence states (*i.e.*, with low electron density compared to their metallic state) favor CO formation. As mentioned above, single-atom catalysts are generally referred as $M^{\delta+}$ catalysts. Positively charged single atom $Ir^{\delta+}$,[142] $Pt^{\delta+}$,[143,144] $Rh^{\delta+}$,[145] $Au^{\delta+}$ (ref. 146) and $Cu^{\delta+}$ (ref. 147) catalysts were recently reported and exhibited enhanced activity in several catalytic reactions such as the water–gas shift reaction and CO oxidation. The electronic properties of a specific metal also can be tuned by controlled doping-segregation in AB_xO_y-type complex oxides such as perovskites, spinels, and mullites. Future efforts should focus on the development of stable and low-cost $M^{\delta+}$ catalysts to attenuate the CO binding energy and therefore enhance the selectivity of the RWGS reaction.

Excitation-induced desorption. In addition to tuning the CO binding energy, other methods may be pursued to enhance CO desorption, such as excitation-induced desorption. In recent decades, photoexcitation-induced CO desorption has been reported by several groups.[148–151] The proper application of these methods may facilitate desorption and inhibit further hydrogenation of adsorbed CO, improving the selectivity toward RWGS.

Competitive adsorption. Recent studies have revealed that water occupies the active metal sites and influences the catalytic performance. Due to the limited number of adsorption sites on the surface of the active metal, the introduction of other strongly-adsorbed species should lead to the desorption of *CO and prohibit its further hydrogenation. The addition of a proper amount of competitively absorbed species should promote the selectivity of the target product.

The determination and controlled synthesis of active sites are necessary to enable the development of active, selective, and stable catalysts for scaling up in industrial processes. For the reduction of CO_2 by H_2, dual-functional catalysts that are active for binding CO_2 and for its subsequent hydrogenation are required. Strong metal–support interactions (SMSIs) and metal–oxide interfaces facilitate these mechanisms,[152] where a support with strong oxygen affinity enhances CO_2 adsorption, and well-dispersed transition metals dissociate H_2, which then spill over onto the support to hydrogenate CO_2.[153–155] Therefore, efforts to improve CO_2 hydrogenation catalysts may aim to characterize the active sites and roles of the metal and the support in order to enable controlled synthesis of more effective catalysts.

SMSIs and bimetallic formation can modify the electronic properties of a catalyst, but these properties may be affected by reaction gas atmosphere and temperature. Therefore, accurate characterization of catalysts under reaction conditions (*in situ* or operando characterization) is crucial for correctly describing the active sites. These accurate descriptions of active sites under reaction conditions can then be used in models (for example, using DFT calculations and Kinetic Monte Carlo simulations) to correlate fundamental descriptors with reaction trends. Furthermore, this characterization is necessary for the identification of appropriate descriptors, such as oxidation state, adsorbed intermediates, and oxygen, CO, or hydrogen binding energy, to be used for predicting more active catalysts. The identification of accurate descriptors through correlating DFT calculations with reaction trends can save significant amounts of catalyst screening time.

The effects of oxide support properties and oxygen exchange on CO_2 activation are significant, but the specific mechanisms are not well understood. The oxygen storage capacity and oxygen mobility in reducible metal oxides, particularly ceria, may favor CO_2 adsorption onto oxygen vacancies and promote C–O bond scission.[156–161] Therefore, future studies may explore the effects of oxygen storage capacity of high surface area reducible metal oxide supports on CO_2 reduction under reaction conditions.

Conflicts of interest

There are no conflicts to declare.

Acknowledgements

Authors from Tsinghua University acknowledge support from the National Natural Science Foundation of China (NSFC) under Grant No. 21978148 and 21673125. Authors from Columbia University acknowledge support from the U.S. Department of Energy (DOE), Office of Basic Energy Sciences, Catalysis Science Program, under Contract No. DE-SC0012704. We would like to thank Dr Qiyuan Wu from Stony Brook University for his suggestions on this perspective article.

References

1 A. A. Lacis, G. A. Schmidt, D. Rind and R. A. Ruedy, Atmospheric CO_2: Principal Control Knob Governing Earth's Temperature, *Science*, 2010, **330**(6002), 356.

2 J. Piñol, J. Terradas and F. Lloret, Climate Warming, Wildfire Hazard, and, Wildfire Occurrence in Coastal Eastern Spain, *Clim. Change*, 1998, **38**(3), 345.

3 M. M. Q. Mirza, Climate change and extreme weather events: can developing countries adapt?, *Clim. Policy*, 2003, **3**(3), 233.

4 D. A. Lashof and D. R. Ahuja, Relative contributions of greenhouse gas emissions to global warming, *Nature*, 1990, **344**(6266), 529.

5 A. A. Lacis, G. A. Schmidt, D. Rind and R. A. Ruedy, Atmospheric CO_2: principal control knob governing Earth's temperature, *Science*, 2010, **330**(6002), 356.

6 P. R. Doose, in *The Geochemical Society Special Publications*, ed. R. J. Hill, J. Leventhal, Z. Aizenshtat, M. J. Baedecker, G. Claypool, R. Eganhouse, M. Goldhaber and K. Peters, Elsevier, 2004, vol. 9.

7 A. Montenegro, K. Zickfeld, M. Eby, D. Archer, K. J. Meissner and A. J. Weaver, Lifetime of Anthropogenic Climate Change: Millennial Time Scales of Potential CO_2 and Surface Temperature Perturbations, *J. Clim.*, 2009, **22**(10), 2501.

8 B. M. Tackett, E. Gomez and J. G. Chen, Net reduction of CO_2 via its thermocatalytic and electrocatalytic transformation reactions in standard and hybrid processes, *Nat. Catal.*, 2019, **2**(5), 381.

9 J. Zhang, Z. Li, Z. Zhang, K. Feng and B. Yan, Can thermocatalytic transformations of captured CO_2 reduce CO_2 emissions?, *Appl. Energy*, 2021, **281**, 116076.

10 G. A. Somorjai and C. J. Kliewer, Reaction selectivity in heterogeneous catalysis, *React. Kinet. Catal. Lett.*, 2009, **96**(2), 191.

11 X. Su, X. F. Yang, Y. Huang, B. Liu and T. Zhang, Single-Atom Catalysis toward Efficient CO_2 Conversion to CO and Formate Products, *Acc. Chem. Res.*, 2019, **52**(3), 656.

12 M. D. Porosoff, B. Yan and J. G. Chen, Catalytic reduction of CO_2 by H2 for synthesis of CO, methanol and hydrocarbons: challenges and opportunities, *Energy Environ. Sci.*, 2016, **9**(1), 62.

13 M. A. A. Aziz, A. A. Jalil, S. Triwahyono and A. Ahmad, CO_2 methanation over heterogeneous catalysts: recent progress and future prospects, *Green Chem.*, 2015, **17**(5), 2647.

14 Y. A. Daza and J. N. Kuhn, CO_2conversion by reverse water gas shift catalysis: comparison of catalysts, mechanisms and their consequences for CO_2conversion to liquid fuels, *RSC Adv.*, 2016, **6**(55), 49675.

15 X. Chen, X. Su, H.-Y. Su, X. Liu, S. Miao, Y. Zhao, K. Sun, Y. Huang and T. Zhang, Theoretical Insights and the Corresponding Construction of Supported Metal Catalysts for Highly Selective CO_2 to CO Conversion, *ACS Catal.*, 2017, **7**(7), 4613.

16 Y. Li, S. H. Chan and Q. Sun, Heterogeneous catalytic conversion of CO_2: a comprehensive theoretical review, *Nanoscale*, 2015, **7**(19), 8663.

17 M. Younas, L. Loong Kong, M. J. K. Bashir, H. Nadeem, A. Shehzad and S. Sethupathi, Recent Advancements, Fundamental Challenges, and Opportunities in Catalytic Methanation of CO_2, *Energy Fuels*, 2016, **30**(11), 8815.

18 W. Wei and G. Jinlong, Methanation of carbon dioxide: an overview, *Front. Chem. Sci. Eng.*, 2011, **5**(1), 2.

19 P. Frontera, A. Macario, M. Ferraro and P. Antonucci, Supported Catalysts for CO_2 Methanation: A Review, *Catalysts*, 2017, **7**(12), 59.

20 W. J. Lee, C. Li, H. Prajitno, J. Yoo, J. Patel, Y. Yang and S. Lim, Recent trend in thermal catalytic low temperature CO_2 methanation: A critical review, *Catal. Today*, 2020, DOI: 10.1016/j.cattod.2020.02.017.

21 A. Solis-Garcia and J. C. Fierro-Gonzalez, Mechanistic Insights into the CO(2) Methanation Catalyzed by Supported Metals: A Review, *J. Nanosci. Nanotechnol.*, 2019, **19**(6), 3110.

22 M. Zhu, Q. Ge and X. Zhu, Catalytic Reduction of CO_2 to CO via Reverse Water Gas Shift Reaction: Recent Advances in the Design of Active and Selective Supported Metal Catalysts, *Trans. Tianjin Univ.*, 2020, **26**(3), 172.

23 X. Su, X. Yang, B. Zhao and Y. Huang, Designing of highly selective and high-temperature endurable RWGS heterogeneous catalysts: recent advances and the future directions, *J. Energy Chem.*, 2017, **26**(5), 854.

24 I. U. Din, M. S. Shaharun, M. A. Alotaibi, A. I. Alharthi and A. Naeem, Recent developments on heterogeneous catalytic CO_2 reduction to methanol, *J. CO2 Util.*, 2019, **34**, 20.

25 R. Guil-Lopez, N. Mota, J. Llorente, E. Millan, B. Pawelec, J. L. G. Fierro and R. M. Navarro, Methanol Synthesis from CO_2: A Review of the Latest Developments in Heterogeneous Catalysis, *Materials*, 2019, **12**(23), 3902.

26 X.-M. Liu, G. Q. Lu, Z.-F. Yan and J. Beltramini, Recent Advances in Catalysts for Methanol Synthesis via Hydrogenation of CO and CO_2, *Ind. Eng. Chem. Res.*, 2003, **42**(25), 6518.

27 M. Bowker, Methanol Synthesis from CO_2 Hydrogenation, *ChemCatChem*, 2019, **11**(17), 4238.

28 S. Kattel, P. Liu and J. G. Chen, Tuning Selectivity of CO_2 Hydrogenation Reactions at the Metal/Oxide Interface, *J. Am. Chem. Soc.*, 2017, **139**(29), 9739.

29 C. Heine, B. A. Lechner, H. Bluhm and M. Salmeron, Recycling of CO_2: Probing the Chemical State of the Ni (111) Surface during the Methanation Reaction with Ambient-Pressure X-Ray Photoelectron Spectroscopy, *J. Am. Chem. Soc.*, 2016, **138**(40), 13246.
30 K. Zhao, L. Wang, M. Calizzi, E. Moioli and A. Züttel, In Situ Control of the Adsorption Species in CO_2 Hydrogenation: Determination of Intermediates and Byproducts, *J. Phys. Chem. C*, 2018, **122**(36), 20888.
31 N. M. Martin, F. Hemmingsson, X. Wang, L. R. Merte, U. Hejral, J. Gustafson, M. Skoglundh, D. M. Meira, A.-C. Dippel, O. Gutowski, *et al.*, Structure–function relationship during CO_2 methanation over Rh/Al2O3 and Rh/SiO2 catalysts under atmospheric pressure conditions, *Catal. Sci. Technol.*, 2018, **8**(10), 2686.
32 J. Resasco, L. DeRita, S. Dai, J. P. Chada, M. Xu, X. Yan, J. Finzel, S. Hanukovich, A. S. Hoffman, G. W. Graham, *et al.*, Uniformity Is Key in Defining Structure-Function Relationships for Atomically Dispersed Metal Catalysts: The Case of Pt/CeO_2, *J. Am. Chem. Soc.*, 2020, **142**(1), 169.
33 L. Zhang, I. A. W. Filot, Y. Q. Su, J. X. Liu and E. J. M. Hensen, Understanding the Impact of Defects on Catalytic CO Oxidation of LaFeO3-Supported Rh, Pd, and Pt Single-Atom Catalysts, *J. Phys. Chem. C*, 2019, **123**(12), 7290.
34 R. Mutschler, E. Moioli, W. Luo, N. Gallandat and A. Züttel, CO_2 hydrogenation reaction over pristine Fe, Co, Ni, Cu and Al2O3 supported Ru: Comparison and determination of the activation energies, *J. Catal.*, 2018, **366**, 139.
35 G. Garbarino, T. Cavattoni, P. Riani and G. Busca, Support effects in metal catalysis: a study of the behavior of unsupported and silica-supported cobalt catalysts in the hydrogenation of CO_2 at atmospheric pressure, *Catal. Today*, 2020, **345**, 213.
36 G. Garbarino, P. Riani, L. Magistri and G. Busca, A study of the methanation of carbon dioxide on Ni/Al2O3 catalysts at atmospheric pressure, *Int. J. Hydrogen Energy*, 2014, **39**(22), 11557.
37 D. Pandey, K. Ray, R. Bhardwaj, S. Bojja, K. V. R. Chary and G. Deo, Promotion of unsupported nickel catalyst using iron for CO_2 methanation, *Int. J. Hydrogen Energy*, 2018, **43**(10), 4987.
38 D. H. Kim, S. W. Han, H. S. Yoon and Y. D. Kim, Reverse water gas shift reaction catalyzed by Fe nanoparticles with high catalytic activity and stability, *J. Ind. Eng. Chem.*, 2015, **23**, 67.
39 M. Bersani, K. Gupta, A. K. Mishra, R. Lanza, S. F. R. Taylor, H.-U. Islam, N. Hollingsworth, C. Hardacre, N. H. de Leeuw and J. A. Darr, Combined EXAFS, XRD, DRIFTS, and DFT Study of Nano Copper-Based Catalysts for CO_2Hydrogenation, *ACS Catal.*, 2016, **6**(9), 5823.
40 P. Panagiotopoulou, Hydrogenation of CO 2 over supported noble metal catalysts, *Appl. Catal., A*, 2017, **542**, 63.
41 A. Beuls, C. Swalus, M. Jacquemin, G. Heyen, A. Karelovic and P. Ruiz, Methanation of CO_2: Further insight into the mechanism over Rh/γ-Al2O3 catalyst, *Appl. Catal., B*, 2012, **113–114**, 2.
42 A. Petala and P. Panagiotopoulou, Methanation of CO_2 over alkali-promoted Ru/TiO2 catalysts: I. Effect of alkali additives on catalytic activity and selectivity, *Appl. Catal., B*, 2018, **224**, 919.
43 S. Tada, O. J. Ochieng, R. Kikuchi, T. Haneda and H. Kameyama, Promotion of CO_2 methanation activity and CH4 selectivity at low temperatures over Ru/CeO_2/Al2O3 catalysts, *Int. J. Hydrogen Energy*, 2014, **39**(19), 10090.
44 T. Avanesian, G. S. Gusmão and P. Christopher, Mechanism of CO_2 reduction by H2 on Ru(0 0 0 1) and general selectivity descriptors for late-transition metal catalysts, *J. Catal.*, 2016, **343**, 86.
45 P. A. U. Aldana, F. Ocampo, K. Kobl, B. Louis, F. Thibault-Starzyk, M. Daturi, P. Bazin, S. Thomas and A. C. Roger, Catalytic CO_2 valorization into CH4 on Ni-based ceria-zirconia. Reaction mechanism by operando IR spectroscopy, *Catal. Today*, 2013, **215**, 201.
46 D. C. D. da Silva, S. Letichevsky, L. E. P. Borges and L. G. Appel, The Ni/ZrO2 catalyst and the methanation of CO and CO_2, *Int. J. Hydrogen Energy*, 2012, **37**(11), 8923.
47 J.-N. Park and E. W. McFarland, A highly dispersed Pd–Mg/SiO2 catalyst active for methanation of CO_2, *J. Catal.*, 2009, **266**(1), 92.
48 R. Zhou, N. Rui, Z. Fan and C.-J. Liu, Effect of the structure of Ni/TiO2 catalyst on CO_2 methanation, *Int. J. Hydrogen Energy*, 2016, **41**(47), 22017.
49 N. M. Martin, P. Velin, M. Skoglundh, M. Bauer and P.-A. Carlsson, Catalytic hydrogenation of CO_2 to methane over supported Pd, Rh and Ni catalysts, *Catal. Sci. Technol.*, 2017, **7**(5), 1086.
50 L. R. Winter, E. Gomez, B. Yan, S. Yao and J. G. Chen, Tuning Ni-catalyzed CO_2 hydrogenation selectivity via Ni-ceria support interactions and Ni-Fe bimetallic formation, *Appl. Catal., B*, 2018, **224**, 442.
51 G. D. Weatherbee and C. H. Bartholomew, Hydrogenation of CO_2 on group VIII metals: IV. Specific activities and selectivities of silica-supported Co, Fe, and Ru, *J. Catal.*, 1984, **87**(2), 352.
52 J. Zhu, G. Zhang, W. Li, X. Zhang, F. Ding, C. Song and X. Guo, Deconvolution of the Particle Size Effect on CO_2 Hydrogenation over Iron-Based Catalysts, *ACS Catal.*, 2020, **10**(13), 7424.
53 X. Chen, X. Su, B. Liang, X. Yang, X. Ren, H. Duan, Y. Huang and T. Zhang, Identification of relevant active sites and a mechanism study for reverse water gas shift reaction over Pt/CeO 2 catalysts, *J. Energy Chem.*, 2016, **25**(6), 1051.
54 S. Kattel, B. Yan, J. G. Chen and P. Liu, CO_2 hydrogenation on Pt, Pt/SiO2 and Pt/TiO2: Importance of synergy between Pt and oxide support, *J. Catal.*, 2016, **343**, 115.

55 S. S. Kim, H. H. Lee and S. C. Hong, A study on the effect of support's reducibility on the reverse water-gas shift reaction over Pt catalysts, *Appl. Catal., A*, 2012, **423–424**, 100.

56 S.-I. Fujita and N. Takezawa, Difference in the selectivity of CO and CO_2 methanation reactions, *Chem. Eng. J.*, 1997, **68**(1), 63.

57 M. A. A. Aziz, A. A. Jalil, S. Triwahyono and S. M. Sidik, Methanation of carbon dioxide on metal-promoted mesostructured silica nanoparticles, *Appl. Catal., A*, 2014, **486**, 115.

58 S. Kattel, B. Yan, Y. Yang, J. G. Chen and P. Liu, Optimizing Binding Energies of Key Intermediates for CO_2 Hydrogenation to Methanol over Oxide-Supported Copper, *J. Am. Chem. Soc.*, 2016, **138**(38), 12440.

59 A. Wang, J. Li and T. Zhang, Heterogeneous single-atom catalysis, *Nat. Rev. Chem.*, 2018, **2**(6), 65.

60 M. Dhiman and V. Polshettiwar, Supported Single Atom and Pseudo-Single Atom of Metals as Sustainable Heterogeneous Nanocatalysts, *ChemCatChem*, 2018, **10**(5), 881.

61 H. Zhao, S. Yao, M. Zhang, F. Huang, Q. Fan, S. Zhang, H. Liu, D. Ma and C. Gao, Ultra-Small Platinum Nanoparticles Encapsulated in Sub-50 nm Hollow Titania Nanospheres for Low-Temperature Water-Gas Shift Reaction, *ACS Appl. Mater. Interfaces*, 2018, **10**(43), 36954.

62 X. Zhao, H. Xu, X. Wang, Z. Zheng, Z. Xu and J. Ge, Monodisperse Metal-Organic Framework Nanospheres with Encapsulated Core-Shell Nanoparticles Pt/Au@Pd@{Co_2(oba)4(3-bpdh)2}4H_2O for the Highly Selective Conversion of CO_2 to CO, *ACS Appl. Mater. Interfaces*, 2018, **10**(17), 15096.

63 X.-F. Yang, A. Wang, B. Qiao, J. Li, J. Liu and T. Zhang, Single-Atom Catalysts: A New Frontier in Heterogeneous Catalysis, *Acc. Chem. Res.*, 2013, **46**(8), 1740.

64 H. Zhang, G. Liu, L. Shi and J. Ye, Single-Atom Catalysts: Emerging Multifunctional Materials in Heterogeneous Catalysis, *Adv. Energy Mater.*, 2018, **8**(1), 1701343.

65 J. H. Kwak, L. Kovarik and J. Szanyi, CO_2 Reduction on Supported Ru/Al2O3 Catalysts: Cluster Size Dependence of Product Selectivity, *ACS Catal.*, 2013, **3**(11), 2449.

66 J. H. Kwak, L. Kovarik and J. Szanyi, Heterogeneous Catalysis on Atomically Dispersed Supported Metals: CO_2 Reduction on Multifunctional Pd Catalysts, *ACS Catal.*, 2013, **3**(9), 2094.

67 A. Aitbekova, L. Wu, C. J. Wrasman, A. Boubnov, A. S. Hoffman, E. D. Goodman, S. R. Bare and M. Cargnello, Low-Temperature Restructuring of CeO_2-Supported Ru Nanoparticles Determines Selectivity in CO_2 Catalytic Reduction, *J. Am. Chem. Soc.*, 2018, **140**(42), 13736.

68 J. C. Matsubu, V. N. Yang and P. Christopher, Isolated metal active site concentration and stability control catalytic CO_2 reduction selectivity, *J. Am. Chem. Soc.*, 2015, **137**(8), 3076.

69 S. Li, Y. Xu, Y. Chen, W. Li, L. Lin, M. Li, Y. Deng, X. Wang, B. Ge, C. Yang, *et al.*, Tuning the Selectivity of Catalytic Carbon Dioxide Hydrogenation over Iridium/Cerium Oxide Catalysts with a Strong Metal-Support Interaction, *Angew. Chem., Int. Ed.*, 2017, **56**(36), 10761.

70 Y. Wang, H. Arandiyan, J. Scott, K.-F. Aguey-Zinsou and R. Amal, Single Atom and Nanoclustered Pt Catalysts for Selective CO_2 Reduction, *ACS Appl. Energy Mater.*, 2018, **1**(12), 6781.

71 H. C. Wu, Y. C. Chang, J. H. Wu, J. H. Lin, I. K. Lin and C. S. Chen, Methanation of CO_2 and reverse water gas shift reactions on Ni/SiO2 catalysts: the influence of particle size on selectivity and reaction pathway, *Catal. Sci. Technol.*, 2015, **5**(8), 4154.

72 B. Lu and K. Kawamoto, Preparation of monodispersed NiO particles in SBA-15, and its enhanced selectivity for reverse water gas shift reaction, *J. Environ. Chem. Eng.*, 2013, **1**(3), 300.

73 B. Lu and K. Kawamoto, Preparation of mesoporous CeO_2 and monodispersed NiO particles in CeO_2, and enhanced selectivity of NiO/CeO_2 for reverse water gas shift reaction, *Mater. Res. Bull.*, 2014, **53**, 70.

74 R. V. Gonçalves, L. L. R. Vono, R. Wojcieszak, C. S. B. Dias, H. Wender, E. Teixeira-Neto and L. M. Rossi, Selective hydrogenation of CO 2 into CO on a highly dispersed nickel catalyst obtained by magnetron sputtering deposition: A step towards liquid fuels, *Appl. Catal., B*, 2017, **209**, 240.

75 C. Vogt, E. Groeneveld, G. Kamsma, M. Nachtegaal, L. Lu, C. J. Kiely, P. H. Berben, F. Meirer and B. M. Weckhuysen, Unravelling structure sensitivity in CO_2 hydrogenation over nickel, *Nat. Catal.*, 2018, **1**(2), 127.

76 Y. Yan, Q. Wang, C. Jiang, Y. Yao, D. Lu, J. Zheng, Y. Dai, H. Wang and Y. Yang, Ru/Al2O3 catalyzed CO_2 hydrogenation: Oxygen-exchange on metal-support interfaces, *J. Catal.*, 2018, **367**, 194.

77 S. Liang, C. Hao and Y. Shi, The Power of Single-Atom Catalysis, *ChemCatChem*, 2015, **7**(17), 2559.

78 Z. Zhang, Y. Zhu, H. Asakura, B. Zhang, J. Zhang, M. Zhou, Y. Han, T. Tanaka, A. Wang, T. Zhang, *et al.*, Thermally stable single atom Pt/m-Al2O3 for selective hydrogenation and CO oxidation, *Nat. Commun.*, 2017, **8**, 16100.

79 P. Panagiotopoulou, Methanation of CO_2 over alkali-promoted Ru/TiO2 catalysts: II. Effect of alkali additives on the reaction pathway, *Appl. Catal., B*, 2018, **236**, 162.

80 P. Chou and M. A. Vannice, Calorimetric heat of adsorption measurements on palladium: I. Influence of crystallite size and support on hydrogen adsorption, *J. Catal.*, 1987, **104**(1), 1.

81 J. Martins, N. Batail, S. Silva, S. Rafik-Clement, A. Karelovic, D. P. Debecker, A. Chaumonnot and D. Uzio, CO_2 hydrogenation with shape-controlled Pd nanoparticles embedded in mesoporous silica: Elucidating stability and selectivity issues, *Catal. Commun.*, 2015, **58**, 11.

82 B. T. Loveless, C. Buda, M. Neurock and E. Iglesia, CO chemisorption and dissociation at high coverages during CO

hydrogenation on Ru catalysts, *J. Am. Chem. Soc.*, 2013, **135**(16), 6107.

83 D. Beierlein, D. Häussermann, M. Pfeifer, T. Schwarz, K. Stöwe, Y. Traa and E. Klemm, Is the CO_2 methanation on highly loaded Ni-Al2O3 catalysts really structure-sensitive?, *Appl. Catal., B*, 2019, **247**, 200.

84 Y. Guo, S. Mei, K. Yuan, D.-J. Wang, H.-C. Liu, C.-H. Yan and Y.-W. Zhang, Low-Temperature CO_2 Methanation over CeO_2-Supported Ru Single Atoms, Nanoclusters, and Nanoparticles Competitively Tuned by Strong Metal–Support Interactions and H-Spillover Effect, *ACS Catal.*, 2018, **8**(7), 6203.

85 Q. Liu, B. Bian, J. Fan and J. Yang, Cobalt doped Ni based ordered mesoporous catalysts for CO_2 methanation with enhanced catalytic performance, *Int. J. Hydrogen Energy*, 2018, **43**(10), 4893.

86 L. Xu, X. Lian, M. Chen, Y. Cui, F. Wang, W. Li and B. Huang, CO_2 methanation over Co Ni bimetal-doped ordered mesoporous Al2O3 catalysts with enhanced low-temperature activities, *Int. J. Hydrogen Energy*, 2018, **43**(36), 17172.

87 H. Arandiyan, Y. Wang, J. Scott, S. Mesgari, H. Dai and R. Amal, In Situ Exsolution of Bimetallic Rh-Ni Nanoalloys: a Highly Efficient Catalyst for CO_2 Methanation, *ACS Appl. Mater. Interfaces*, 2018, **10**(19), 16352.

88 X. Shang, D. Deng, X. Wang, W. Xuan, X. Zou, W. Ding and X. Lu, Enhanced low-temperature activity for CO_2 methanation over Ru doped the Ni/CexZr(1−)O2 catalysts prepared by one-pot hydrolysis method, *Int. J. Hydrogen Energy*, 2018, **43**(14), 7179.

89 Q. Liu, S. Wang, G. Zhao, H. Yang, M. Yuan, X. An, H. Zhou, Y. Qiao and Y. Tian, CO_2 methanation over ordered mesoporous NiRu-doped CaO-Al2O3 nanocomposites with enhanced catalytic performance, *Int. J. Hydrogen Energy*, 2018, **43**(1), 239.

90 T. Burger, F. Koschany, O. Thomys, K. Köhler and O. Hinrichsen, CO_2 methanation over Fe- and Mn-promoted co-precipitated Ni-Al catalysts: Synthesis, characterization and catalysis study, *Appl. Catal., A*, 2018, **558**, 44.

91 H. Lu, X. Yang, G. Gao, J. Wang, C. Han, X. Liang, C. Li, Y. Li, W. Zhang and X. Chen, Metal (Fe, Co, Ce or La) doped nickel catalyst supported on ZrO2 modified mesoporous clays for CO and CO_2 methanation, *Fuel*, 2016, **183**, 335.

92 C. Mebrahtu, F. Krebs, S. Perathoner, S. Abate, G. Centi and R. Palkovits, Hydrotalcite based Ni–Fe/(Mg, Al)Ox catalysts for CO_2 methanation – tailoring Fe content for improved CO dissociation, basicity, and particle size, *Catal. Sci. Technol.*, 2018, **8**(4), 1016.

93 B. Mutz, M. Belimov, W. Wang, P. Sprenger, M.-A. Serrer, D. Wang, P. Pfeifer, W. Kleist and J.-D. Grunwaldt, Potential of an Alumina-Supported Ni3Fe Catalyst in the Methanation of CO_2: Impact of Alloy Formation on Activity and Stability, *ACS Catal.*, 2017, **7**(10), 6802.

94 B. Yan, B. Zhao, S. Kattel, Q. Wu, S. Yao, D. Su and J. G. Chen, Tuning CO_2 hydrogenation selectivity via metal-oxide interfacial sites, *J. Catal.*, 2019, **374**, 60.

95 M. Mihet and M. D. Lazar, Methanation of CO_2 on Ni/γ-Al2O3: Influence of Pt, Pd or Rh promotion, *Catal. Today*, 2018, **306**, 294.

96 S. K. Beaumont, S. Alayoglu, C. Specht, W. D. Michalak, V. V. Pushkarev, J. Guo, N. Kruse and G. A. Somorjai, Combining in situ NEXAFS spectroscopy and CO(2) methanation kinetics to study Pt and Co nanoparticle catalysts reveals key insights into the role of platinum in promoted cobalt catalysis, *J. Am. Chem. Soc.*, 2014, **136**(28), 9898.

97 S. K. Beaumont, S. Alayoglu, C. Specht, N. Kruse and G. A. Somorjai, A nanoscale demonstration of hydrogen atom spillover and surface diffusion across silica using the kinetics of CO_2 methanation catalyzed on spatially separate Pt and Co nanoparticles, *Nano Lett.*, 2014, **14**(8), 4792.

98 Z. Ou, C. Qin, J. Niu, L. Zhang and J. Ran, A comprehensive DFT study of CO_2 catalytic conversion by H2 over Pt-doped Ni catalysts, *Int. J. Hydrogen Energy*, 2019, **44**(2), 819.

99 M. C. Bacariza, R. Bértolo, I. Graça, J. M. Lopes and C. Henriques, The effect of the compensating cation on the catalytic performances of Ni/USY zeolites towards CO_2 methanation, *J. CO2 Util.*, 2017, **21**, 280.

100 R. Büchel, A. Baiker and S. E. Pratsinis, Effect of Ba and K addition and controlled spatial deposition of Rh in Rh/Al2O3 catalysts for CO_2 hydrogenation, *Appl. Catal., A*, 2014, **477**, 93.

101 D. Heyl, U. Rodemerck and U. Bentrup, Mechanistic Study of Low-Temperature CO_2 Hydrogenation over Modified Rh/Al2O3 Catalysts, *ACS Catal.*, 2016, **6**(9), 6275.

102 M. D. Porosoff, J. W. Baldwin, X. Peng, G. Mpourmpakis and H. D. Willauer, Potassium-Promoted Molybdenum Carbide as a Highly Active and Selective Catalyst for CO_2 Conversion to CO, *ChemSusChem*, 2017, **10**(11), 2408.

103 B. Liang, H. Duan, X. Su, X. Chen, Y. Huang, X. Chen, J. J. Delgado and T. Zhang, Promoting role of potassium in the reverse water gas shift reaction on Pt/mullite catalyst, *Catal. Today*, 2017, **281**, 319.

104 X. Yang, X. Su, X. Chen, H. Duan, B. Liang, Q. Liu, X. Liu, Y. Ren, Y. Huang and T. Zhang, Promotion effects of potassium on the activity and selectivity of Pt/zeolite catalysts for reverse water gas shift reaction, *Appl. Catal., B*, 2017, **216**, 95.

105 J. A. H. Dreyer, P. Li, L. Zhang, G. K. Beh, R. Zhang, P. H. L. Sit and W. Y. Teoh, Influence of the oxide support reducibility on the CO_2 methanation over Ru-based catalysts, *Appl. Catal., B*, 2017, **219**, 715.

106 J. Díez-Ramírez, P. Sánchez, V. Kyriakou, S. Zafeiratos, G. E. Marnellos, M. Konsolakis and F. Dorado, Effect of support nature on the cobalt-catalyzed CO_2 hydrogenation, *J. CO2 Util.*, 2017, **21**, 562.

107 H. Muroyama, Y. Tsuda, T. Asakoshi, H. Masitah, T. Okanishi, T. Matsui and K. Eguchi, Carbon dioxide methanation over Ni catalysts supported on various metal oxides, *J. Catal.*, 2016, **343**, 178.

108 L. R. Winter, R. Chen, X. Chen, K. Chang, Z. Liu, S. D. Senanayake, A. M. Ebrahim and J. G. Chen, Elucidating the roles of metallic Ni and oxygen vacancies in CO_2 hydrogenation over Ni/CeO_2 using isotope exchange and in situ measurements, *Appl. Catal., B*, 2019, **245**, 360.

109 A. Lechkar, A. Barroso Bogeat, G. Blanco, J. M. Pintado and M. Soussi el Begrani, Methanation of carbon dioxide over ceria-praseodymia promoted Ni-alumina catalysts. Influence of metal loading, promoter composition and alumina modifier, *Fuel*, 2018, **234**, 1401.

110 J. Lin, C. Ma, Q. Wang, Y. Xu, G. Ma, J. Wang, H. Wang, C. Dong, C. Zhang and M. Ding, Enhanced low-temperature performance of CO_2 methanation over mesoporous Ni/Al2O3-ZrO2 catalysts, *Appl. Catal., B*, 2019, **243**, 262.

111 F. Meng, Z. Li, F. Ji and M. Li, Effect of ZrO2 on catalyst structure and catalytic methanation performance over Ni-based catalyst in slurry-bed reactor, *Int. J. Hydrogen Energy*, 2015, **40**(29), 8833.

112 W. Nie, X. Zou, X. Shang, X. Wang, W. Ding and X. Lu, CeO 2 -assisted Ni nanocatalysts supported on mesoporous γ-Al 2 O 3 for the production of synthetic natural gas, *Fuel*, 2017, **202**, 135.

113 I. Iglesias, A. Quindimil, F. Mariño, U. De-La-Torre and J. R. González-Velasco, Zr promotion effect in CO_2 methanation over ceria supported nickel catalysts, *Int. J. Hydrogen Energy*, 2019, **44**(3), 1710.

114 G. Zhou, H. Liu, K. Cui, A. Jia, G. Hu, Z. Jiao, Y. Liu and X. Zhang, Role of surface Ni and Ce species of Ni/CeO_2 catalyst in CO_2 methanation, *Appl. Surf. Sci.*, 2016, **383**, 248.

115 X. Nie, H. Wang, W. Li, Y. Chen, X. Guo and C. Song, DFT insight into the support effect on the adsorption and activation of key species over Co catalysts for CO_2 methanation, *J. CO2 Util.*, 2018, **24**, 99.

116 Q. Pan, J. Peng, T. Sun, D. Gao, S. Wang and S. Wang, CO_2 methanation on Ni/Ce0.5Zr0.5O2 catalysts for the production of synthetic natural gas, *Fuel Process. Technol.*, 2014, **123**, 166.

117 Q. Pan, J. Peng, S. Wang and S. Wang, In situ FTIR spectroscopic study of the CO_2methanation mechanism on Ni/Ce0.5Zr0.5O2, *Catal. Sci. Technol.*, 2014, **4**(2), 502.

118 F.-M. Sun, C.-F. Yan, Z.-D. Wang, C.-Q. Guo and S.-L. Huang, Ni/Ce–Zr–O catalyst for high CO_2 conversion during reverse water gas shift reaction (RWGS), *Int. J. Hydrogen Energy*, 2015, **40**(46), 15985.

119 X. Liu, C. Kunkel, P. Ramírez de la Piscina, N. Homs, F. Viñes and F. Illas, Effective and Highly Selective CO Generation from CO_2Using a Polycrystalline α-Mo2C Catalyst, *ACS Catal.*, 2017, **7**(7), 4323.

120 H.-S. Na, J.-O. Shim, S.-Y. Ahn, W.-J. Jang, K.-W. Jeon, H.-M. Kim, Y.-L. Lee, K.-J. Kim and H.-S. Roh, Effect of precipitation sequence on physicochemical properties of CeO_2 support for hydrogen production from low-temperature water-gas shift reaction, *Int. J. Hydrogen Energy*, 2018, **43**(37), 17718.

121 T. Sakpal and L. Lefferts, Structure-dependent activity of CeO_2 supported Ru catalysts for CO_2 methanation, *J. Catal.*, 2018, **367**, 171.

122 Q. Lin, X. Y. Liu, Y. Jiang, Y. Wang, Y. Huang and T. Zhang, Crystal phase effects on the structure and performance of ruthenium nanoparticles for CO_2 hydrogenation, *Catal. Sci. Technol.*, 2014, **4**(7), 2058.

123 A. Kim, C. Sanchez, G. Patriarche, O. Ersen, S. Moldovan, A. Wisnet, C. Sassoye and D. P. Debecker, Selective CO_2 methanation on Ru/TiO2 catalysts: unravelling the decisive role of the TiO2 support crystal structure, *Catal. Sci. Technol.*, 2016, **6**(22), 8117.

124 A. Kim, D. P. Debecker, F. Devred, V. Dubois, C. Sanchez and C. Sassoye, CO_2 methanation on Ru/TiO2 catalysts: On the effect of mixing anatase and rutile TiO2 supports, *Appl. Catal., B*, 2018, **220**, 615.

125 Y. Lin, Y. Zhu, X. Pan and X. Bao, Modulating the methanation activity of Ni by the crystal phase of TiO2, *Catal. Sci. Technol.*, 2017, **7**(13), 2813.

126 E. S. Gnanakumar, N. Chandran, I. V. Kozhevnikov, A. Grau-Atienza, E. V. Ramos Fernández, A. Sepulveda-Escribano and N. R. Shiju, Highly efficient nickel-niobia composite catalysts for hydrogenation of CO_2 to methane, *Chem. Eng. Sci.*, 2019, **194**, 2.

127 K. Zhao, W. Wang and Z. Li, Highly efficient Ni/ZrO2 catalysts prepared via combustion method for CO_2 methanation, *J. CO2 Util.*, 2016, **16**, 236.

128 Y. Zhang, Z. Zhang, X. Yang, R. Wang, H. Duan, Z. Shen, L. Li, Y. Su, R. Yang, Y. Zhang, *et al.*, Tuning selectivity of CO_2 hydrogenation by modulating the strong metal–support interaction over Ir/TiO2 catalysts, *Green Chem.*, 2020, **22**(20), 6855–6861.

129 R. Lippi, S. C. Howard, H. Barron, C. D. Easton, I. C. Madsen, L. J. Waddington, C. Vogt, M. R. Hill, C. J. Sumby, C. J. Doonan, *et al.*, Highly active catalyst for CO_2 methanation derived from a metal organic framework template, *J. Mater. Chem. A*, 2017, **5**(25), 12990.

130 Z.-W. Zhao, X. Zhou, Y.-N. Liu, C.-C. Shen, C.-Z. Yuan, Y.-F. Jiang, S.-J. Zhao, L.-B. Ma, T.-Y. Cheang and A.-W. Xu, Ultrasmall Ni nanoparticles embedded in Zr-based MOFs provide high selectivity for CO_2 hydrogenation to methane at low temperatures, *Catal. Sci. Technol.*, 2018, **8**(12), 3160.

131 E. Lam, J. J. Corral-Perez, K. Larmier, G. Noh, P. Wolf, A. Comas-Vives, A. Urakawa and C. Coperet, CO_2 Hydrogenation on Cu/Al2 O3 : Role of the Metal/Support Interface in Driving Activity and Selectivity of a Bifunctional Catalyst, *Angew. Chem., Int. Ed.*, 2019, **58**(39), 13989.

132 F. Liao, Y. Huang, J. Ge, W. Zheng, K. Tedsree, P. Collier, X. Hong and S. C. Tsang, Morphology-dependent interactions of ZnO with Cu nanoparticles at the materials' interface in selective hydrogenation of CO_2 to CH3OH, *Angew. Chem., Int. Ed.*, 2011, **50**(9), 2162.

133 X. Yang, S. Kattel, S. D. Senanayake, J. A. Boscoboinik, X. Nie, J. Graciani, J. A. Rodriguez, P. Liu, D. J. Stacchiola and J. G. Chen, Low Pressure CO_2 Hydrogenation to

Methanol over Gold Nanoparticles Activated on a CeOx/TiO2 Interface, *J. Am. Chem. Soc.*, 2015, **137**(32), 10104.
134 C. Kim, S. Hyeon, J. Lee, W. D. Kim, D. C. Lee, J. Kim and H. Lee, Energy-efficient CO_2 hydrogenation with fast response using photoexcitation of CO_2 adsorbed on metal catalysts, *Nat. Commun.*, 2018, **9**(1), 3027.
135 L. Lin, K. Wang, K. Yang, X. Chen, X. Fu and W. Dai, The visible-light-assisted thermocatalytic methanation of CO_2 over Ru/TiO(2-x)Nx, *Appl. Catal., B*, 2017, **204**, 440.
136 B. Zhao, B. Yan, Z. Jiang, S. Yao, Z. Liu, Q. Wu, R. Ran, S. D. Senanayake, D. Weng and J. G. Chen, High selectivity of CO_2 hydrogenation to CO by controlling the valence state of nickel using perovskite, *Chem. Commun.*, 2018, **54**(53), 7354.
137 A. M. Abdel-Mageed, S. Eckle and R. J. Behm, High Selectivity of Supported Ru Catalysts in the Selective CO Methanation-Water Makes the Difference, *J. Am. Chem. Soc.*, 2015, **137**(27), 8672.
138 H. Arandiyan, K. Kani, Y. Wang, B. Jiang, J. Kim, M. Yoshino, M. Rezaei, A. E. Rowan, H. Dai and Y. Yamauchi, Highly Selective Reduction of Carbon Dioxide to Methane on Novel Mesoporous Rh Catalysts, *ACS Appl. Mater. Interfaces*, 2018, **10**(30), 24963.
139 N. Liu, M. Xu, Y. Yang, S. Zhang, J. Zhang, W. Wang, L. Zheng, S. Hong and M. Wei, Auδ−–Ov–Ti3+ Interfacial Site: Catalytic Active Center toward Low-Temperature Water Gas Shift Reaction, *ACS Catal.*, 2019, **9**(4), 2707.
140 H. Tang, Y. Su, B. Zhang, A. F. Lee, M. A. Isaacs, K. Wilson, L. Li, Y. Ren, J. Huang, M. Haruta, *et al.*, Classical strong metal–support interactions between gold nanoparticles and titanium dioxide, *Sci. Adv.*, 2017, **3**(10), e1700231.
141 X. Zhang, P. Yan, B. Zhao and Z. C. Zhang, Identification of electron-rich mononuclear Ni atoms on TiO2-A distinguished from Ni particles on TiO2-R in guaiacol hydrodeoxygenation pathways, *Catal. Sci. Technol.*, 2020, DOI: 10.1039/d0cy01720e, DOI: 10.1039/d0cy01720e.
142 J. Lin, A. Wang, B. Qiao, X. Liu, X. Yang, X. Wang, J. Liang, J. Li, J. Liu and T. Zhang, Remarkable performance of Ir1/FeO(x) single-atom catalyst in water gas shift reaction, *J. Am. Chem. Soc.*, 2013, **135**(41), 15314.
143 Y. Chen, S. Ji, W. Sun, W. Chen, J. Dong, J. Wen, J. Zhang, Z. Li, L. Zheng, C. Chen, *et al.*, Discovering Partially Charged Single-Atom Pt for Enhanced Anti-Markovnikov Alkene Hydrosilylation, *J. Am. Chem. Soc.*, 2018, **140**(24), 7407.
144 H. Wei, X. Liu, A. Wang, L. Zhang, B. Qiao, X. Yang, Y. Huang, S. Miao, J. Liu and T. Zhang, FeOx-supported platinum single-atom and pseudo-single-atom catalysts for chemoselective hydrogenation of functionalized nitroarenes, *Nat. Commun.*, 2014, **5**, 5634.
145 R. Lang, T. Li, D. Matsumura, S. Miao, Y. Ren, Y. T. Cui, Y. Tan, B. Qiao, L. Li, A. Wang, *et al.*, Hydroformylation of Olefins by a Rhodium Single-Atom Catalyst with Activity Comparable to RhCl(PPh3)3, *Angew. Chem., Int. Ed.*, 2016, **55**(52), 16054.
146 B. Qiao, J.-X. Liang, A. Wang, C.-Q. Xu, J. Li, T. Zhang and J. J. Liu, Ultrastable single-atom gold catalysts with strong covalent metal-support interaction (CMSI), *Nano Res.*, 2015, **8**(9), 2913.
147 A. M. Abdel-Mageed, B. Rungtaweevoranit, M. Parlinska-Wojtan, X. Pei, O. M. Yaghi and R. J. Behm, Highly Active and Stable Single-Atom Cu Catalysts Supported by a Metal-Organic Framework, *J. Am. Chem. Soc.*, 2019, **141**(13), 5201.
148 A. Peremans, K. Fukutani, K. Mase and Y. Murata, CO and CO+ photodesorption from Pt(001) at 193 nm, *Phys. Rev. B: Condens. Matter Mater. Phys.*, 1993, **47**(7), 4135.
149 X. Guo, J. Yoshinobu and J. T. Yates, Photon–induced desorption of CO chemisorbed on the oxidized Ni(111) surface, *J. Chem. Phys.*, 1990, **92**(7), 4320.
150 H. Nakatsuji, H. Morita, H. Nakai, Y. Murata and K. Fukutani, Theoretical study on the photostimulated desorption of CO from a Pt surface, *J. Chem. Phys.*, 1996, **104**(2), 714.
151 H. Aizawa and S. Tsuneyuki, First-principles investigation of photo-induced desorption of CO and NO from Pt(111), *Surf. Sci.*, 1996, **363**(1), 223.
152 J. A. Rodriguez, P. Liu, D. J. Stacchiola, S. D. Senanayake, M. G. White and J. G. Chen, Hydrogenation of CO_2 to Methanol: Importance of Metal–Oxide and Metal–Carbide Interfaces in the Activation of CO_2, *ACS Catal.*, 2015, **5**(11), 6696.
153 D. Duprez, in *Studies in Surface Science and Catalysis*, ed. C. Li and Q. Xin, Elsevier, 1997, vol. 112.
154 S. Kattel, B. Yan, Y. Yang, J. G. Chen and P. Liu, Optimizing Binding Energies of Key Intermediates for CO_2 Hydrogenation to Methanol over Oxide-Supported Copper, *J. Am. Chem. Soc.*, 2016, **138**(38), 12440.
155 X. Wang, H. Shi, J. H. Kwak and J. Szanyi, Mechanism of CO_2 Hydrogenation on Pd/Al2O3 Catalysts: Kinetics and Transient DRIFTS-MS Studies, *ACS Catal.*, 2015, **5**(11), 6337.
156 T. Jin, T. Okuhara, G. J. Mains and J. M. White, Temperature-programmed desorption of carbon monoxide and carbon dioxide from platinum/ceria: an important role for lattice oxygen in carbon monoxide oxidation, *J. Phys. Chem.*, 1987, **91**(12), 3310.
157 C. E. Hori, H. Permana, K. Y. S. Ng, A. Brenner, K. More, K. M. Rahmoeller and D. Belton, Thermal stability of oxygen storage properties in a mixed CeO_2-ZrO2 system, *Appl. Catal., B*, 1998, **16**(2), 105.
158 C. E. Hori, A. Brenner, K. Y. Simon Ng, K. M. Rahmoeller and D. Belton, Studies of the oxygen release reaction in the platinum–ceria–zirconia system, *Catal. Today*, 1999, **50**(2), 299.
159 F. Dong, A. Suda, T. Tanabe, Y. Nagai, H. Sobukawa, H. Shinjoh, M. Sugiura, C. Descorme and D. Duprez, Dynamic oxygen mobility and a new insight into the role

of Zr atoms in three-way catalysts of Pt/CeO_2–ZrO2, *Catal. Today*, 2004, **93–95**, 827.
160 E. M. Sadovskaya, Y. A. Ivanova, L. G. Pinaeva, G. Grasso, T. G. Kuznetsova, A. van Veen, V. A. Sadykov and C. Mirodatos, Kinetics of Oxygen Exchange over CeO_2–ZrO2 Fluorite-Based Catalysts, *J. Phys. Chem. A*, 2007, **111**(20), 4498.
161 A. Bueno-López, K. Krishna and M. Makkee, Oxygen exchange mechanism between isotopic CO_2 and Pt/CeO_2, *Appl. Catal., A*, 2008, **342**(1), 144.